2

Mathematical Modelling of the Turbomachine Flow Path Elements

2.1 Equations of State

The equation of state can be written in different forms depending on the independent variables taken. Numerical algorithms should allow to calculate and optimize the axial turbine stages, both with an ideal and a real working fluid. It uses a single method of calculating the parameters of the state of the working fluid, in which as the independent variables are taken enthalpy *i* and pressure *P*:

$$T = T(P, i); \quad \rho = \rho(P, i); \quad S = S(P, i). \tag{2.1}$$

For a perfect gas equation of state with *P* and *i* variables are very simple:

$$T = \frac{1}{C_p} i; \quad \rho = \frac{C_p}{R} \frac{P}{i}; \quad S = S_0 + C_p \ln i - R \ln P. \tag{2.2}$$

For the water steam approximation formula proposed in [7] is used, which established a procedure to calculate parameters of superheated and wet fluid.

It is easy to verify that the knowledge of the value of the velocity coefficient $\psi = w/w_T$ allows to determine the value of losses at the expansion $i - i_T = \frac{1-\psi^2}{\psi^2} w^2 \Big/ 2$ and obtain an expression that relates the enthalpies i_T and *i* at the end of the isentropic and the actual process of expansion, as well as stagnated enthalpy in relative motion $i_w^* = H + u^2/2 = i + w^2/2$:

$$\left(1 - \psi^2\right) i_w^2 - i + \psi^2 i_T = 0. \tag{2.3}$$

The last expression in combination with isentropic process equation from point 1 with parameters P_1, i_1 and the value of the relative velocity

$$S(P_1, i_1) = S\left(P_{w1}^*, i_{w1}^*\right) = S\left(P, i_T\right). \tag{2.4}$$

allows to come, deleting from (2.3), for example i_T, to the following process equation with unknowns *P*, *i*:

$$S\left(P, \frac{1}{\psi^2}\left[i-\left(1-\psi^2\right)i_w^*\right]\right)-S\left(P_{w1}^*, i_{w1}^*\right)=0\,. \tag{2.5}$$

With the help of the equation (2.5) can be solved a number of problems related to the thermal calculations of stages, which statement depends on which parameter of the unknown is a given. If we assume a known specific enthalpy *i* at the end of expansion, we obtain the equation (2.5) relative to the pressure *P*. This problem arises, for example, based on a predetermined degree of reaction or determining the counter pressure by the theoretical enthalpy drop per stage.

Solution of equations of the form (2.5) with one unknown is carried out by means of minimizing the residual square using one-dimensional search of extreme.

2.2 Aerodynamic Models

2.2.1 Axisymmetric Flow in the Axial Turbine Stage

Assume that in the flow path of the turbine:

- the flow is steady relatively to the impeller, rotating at a constant angular velocity ω about the *z*-axis or stationary guide vanes.
- the fluid is compressible, non-viscous and not thermally conductive, and the effect of viscous forces is taken into account in the form of heat recovery in the energy and the process equations, i.e., friction losses are accounted energetically.
- if the working fluid is real (wet steam) it is considered the equilibrium process of expansion.

- the flow is axisymmetric, i.e., its parameters are independent of the circumferential coordinate.

Under these assumptions the system of equations describing the steady axisymmetric compressible flow motion, includes:

1. The equation of motion in the relative coordinate system in the Crocco form

$$-\vec{W}\times\left[\nabla\times\vec{W}\right]+2\vec{\omega}\times\vec{W}=T\nabla S-\nabla H+\vec{F}+\vec{f}\,, \tag{2.6}$$

where $H=i+w^2/2-u^2/2=i+c^2/2-uc_u$ – rothalpy; $\vec{F}$ – blade force; $\vec{f}=-\vec{W}\dfrac{T}{w^2}\left(\vec{W},\nabla S\right)$ – friction force.

2. Continuity equation

$$\nabla\left(\chi\rho\vec{W}\right)=0\,, \tag{2.7}$$

where χ – blockage factor.

3. The equation of the process or system of equations describing the process

$$\left.\begin{array}{c}\left(1-\psi^2\right)\left(H+u^2/2\right)-i+\psi^2 i_T=0;\\ S_{in}-S_T\left(P,i_T\right)=0.\end{array}\right\} \tag{2.8}$$

4. The equations of state

$$T=T\left(P,i\right);\quad \rho=\rho\left(P,i\right);\quad S=S\left(P,i\right). \tag{2.9}$$

5. The equation of the flow surface

$$\left(\vec{W},\vec{n}\right)=0\,, \tag{2.10}$$

where $\vec{n}$ – normal to the S_2 surface (Fig. 2.1).

6. The equation of blade force orthogonality to the flow surface

$$\left[\vec{n}, \vec{F}\right] = 0. \tag{2.11}$$

Projections of the vortex in the relative motion $\mathrm{rot}\,\vec{W} = \nabla \times \vec{W}$ to be determined by the formulas:

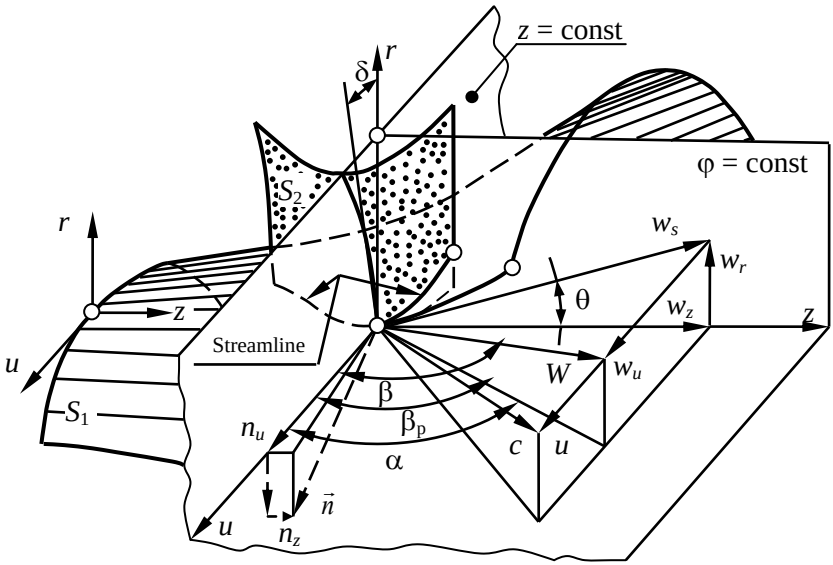

Figure 2.1 *The surfaces of the three-dimensional flow, relative flow angles and velocity components.*

$$\left.\begin{aligned} \mathrm{rot}_r\,\vec{W} &= \frac{1}{r}\left(\frac{\partial w_z}{\partial \phi} - \frac{\partial\left(r w_u\right)}{\partial z}\right); \\ \mathrm{rot}_u\,\vec{W} &= \frac{\partial w_r}{\partial z} - \frac{\partial w_z}{\partial r}; \\ \mathrm{rot}_z\,\vec{W} &= \frac{1}{r}\left(\frac{\partial\left(r w_u\right)}{\partial r} - \frac{\partial w_r}{\partial \phi}\right). \end{aligned}\right\} \tag{2.12}$$

Taking into account (2.12), projection of the equation of motion (2.6) on the axes of cylindrical coordinate system can be written as follows:

- on the *r* axis (radial equilibrium equation)

$$-\frac{w_u}{r}\frac{\partial(rw_u)}{\partial r}-w_z\left(\frac{\partial w_r}{\partial z}-\frac{\partial w_z}{\partial z}\right)-2\omega w_u=T\frac{\partial S}{\partial r}-\frac{\partial H}{\partial r}+F_r+f_r; \qquad (2.13)$$

- on the *u* axis:

$$\frac{w_r}{r}\frac{\partial(rw_u)}{\partial r}+w_z\frac{\partial w_u}{\partial z}+2\omega w_r=F_u+f_u; \qquad (2.14)$$

- instead of the projection on the *z* axis will use energy conservation equation:

$$\frac{\partial H}{\partial s}=0. \qquad (2.15)$$

The components of the relative velocity based on the designated flow angles (Fig. 2.1) can be written as

$$\left.\begin{aligned} w_z &= w_s\cos\theta = w\sin\beta\cos\theta;\\ w_u &= w_s\operatorname{ctg}\beta = w\cos\beta;\\ w_r &= w_s\sin\theta = w\sin\beta\sin\theta. \end{aligned}\right\} \qquad (2.16)$$

From the relation $\left[\vec{n},\vec{F}\right]=0$ will have:

$$n_rF_u=n_uF_r;\quad n_zF_u=n_uF_z;\quad n_zF_r=n_rF_z.$$

We express the ratio of the normals projections through the flow angles (Fig. 2.2):

$$\operatorname{tg}\delta=-\frac{n_r}{n_u};\quad \operatorname{tg}\theta=-\frac{n_z}{n_r};\quad c\operatorname{tg}\beta_p=\frac{n_z}{n_u}.$$

Than we can write

$$F_r=-\operatorname{tg}\delta F_u;\quad F_z=-\operatorname{tg}\theta F_r;\quad F_z=-c\operatorname{tg}\beta_pF_u. \qquad (2.17)$$

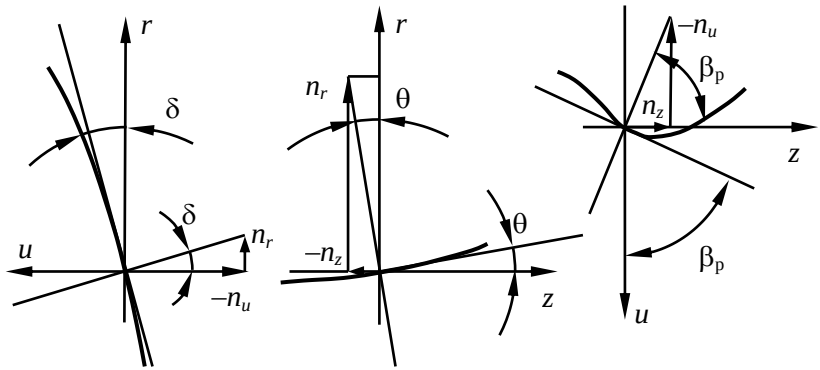

Figure 2.2 *The normal projections to the* S_2 *surface.*

Transforming the radial equilibrium equation

Using the relationship between the coordinates *z*, *r* and *s*, *r* in the meridian plane $\frac{\partial}{\partial z} = \frac{1}{\cos\theta}\left(\frac{\partial}{\partial s} - \sin\theta\frac{\partial}{\partial r}\right)$, and the ratio (2.16), the second term of the equation of radial equilibrium (2.13) can be converted

$$w_z\left(\frac{\partial w_r}{\partial z} - \frac{\partial w_z}{\partial r}\right) = w_s^2\left(\aleph\cos\theta + \sin\theta\frac{\partial \ln w_s}{\partial s} - \frac{\partial \ln w_s}{\partial r}\right). \qquad (2.18)$$

where $\aleph = \partial\theta/\partial s$ – the curvature of the meridian stream line.

To determine the $\partial \ln w_s/\partial s$ member use the continuity equation for an axisymmetric flow:

$$\frac{\partial\left(r\rho\chi w_r\right)}{\partial r} + \frac{\partial\left(r\rho\chi w_z\right)}{\partial z} = 0; \qquad (2.19)$$

which by means of (2.16) and the connecting relations between the cylindrical system of coordinates *z*, *r* and the coordinates of *s*, *n* in the natural grid (stream line *s* in the meridian plane and normal to it *n*)

$$\frac{\partial}{\partial z}=\frac{\partial}{\partial s}\cos\theta-\frac{\partial}{\partial n}\sin\theta,\quad \frac{\partial}{\partial r}=\frac{\partial}{\partial s}\sin\theta-\frac{\partial}{\partial n}\cos\theta$$

transformed into

$$\frac{\partial\theta}{\partial n}+\frac{\partial}{\partial s}\ln\left(\chi r\rho w_s\right)=0\,.$$

The last expression, in turn, by shifting from the coordinates *s*, *n* to coordinates *s*, *r* is represented as:

$$\frac{\cos\theta}{r}\frac{\partial\left(r\mathrm{tg}\,\theta\right)}{\partial r}-\aleph\mathrm{tg}\,\theta+\frac{\partial\ln\chi}{\partial s}+\frac{\partial\ln\rho}{\partial s}+\frac{\partial\ln w_s}{\partial s}=0\,,\qquad(2.20)$$

since

$$\frac{\partial\theta}{\partial n}=\frac{1}{\cos\theta}\left[\frac{\partial\theta}{\partial r}-\sin\theta\frac{\partial\theta}{\partial s}\right]=\frac{1}{\cos\theta}\frac{\partial\theta}{\partial r}-\aleph\mathrm{tg}\,\theta\,.$$

To determine the $\partial\ln\rho/\partial s$ member, engage the energy equation (2.15), where, according to (2.6) and Fig. 2.1

$$H=i+\frac{c^2}{2}-uc_u=i+\frac{c_u^2}{2}+\frac{w_s^2}{2}-uc_u=\mathrm{const}\,.$$

Then we have

$$\frac{\partial i}{\partial s}+c\frac{\partial c}{\partial s}-\frac{\partial\left(uc_u\right)}{\partial s}=\frac{\partial i}{\partial s}+w_s^2\frac{\partial\ln w_s}{\partial s}+c_u\frac{\partial c_u}{\partial s}-\frac{\partial\left(uc_u\right)}{\partial s}\,.\qquad(2.21)$$

The expression for $\partial i/\partial s$ defined differently depending on whether we are dealing with an ideal or a real working fluid.

The first term of (2.13) with (2.16), as well as Fig. 2.1 can be written as:

$$-\frac{w_u}{r}\frac{\partial(rw_u)}{\partial r}=-\frac{w_s^2\mathrm{ctg}^2\beta}{r}-w_s\mathrm{ctg}^2\beta\frac{\partial w_s}{\partial r}-\frac{w_s^2}{2}\frac{\partial\mathrm{ctg}^2\beta}{\partial r};$$

$$-\frac{w_u}{r}\frac{\partial(rw_u)}{\partial r}=-\frac{c_u r-\omega r^2}{r^2}\frac{\partial(c_u r)}{\partial r}+2\omega\frac{c_u r-\omega r^2}{r}.$$

Radial equilibrium equation (2.13) can now be converted to the form:

- *for a given* $c_u r$ (inverse problem):

$$w_s^2\left(\aleph\cos\theta+\sin\theta\frac{\partial\ln w_s}{\partial s}-\frac{\partial\ln w_s}{\partial r}\right)-$$
$$-\frac{c_u r-\omega r^2}{r^2}\frac{\partial(c_u r)}{\partial r}=T\frac{\partial S}{\partial r}-\frac{\partial H}{\partial r}+F_r+f_r; \qquad (2.22)$$

- in the gap between vanes (free channel):

$$w_s^2\left(\aleph\cos\theta+\sin\theta\frac{\partial\ln w_s}{\partial s}-\frac{\partial\ln w_s}{\partial r}\right)=$$
$$=-\frac{c_u r-\omega r^2}{r^2}\frac{\partial(c_u r)}{\partial r}+T\frac{\partial S}{\partial r}-\frac{\partial H}{\partial r}; \qquad (2.23)$$

- for a given β:

$$w_s^2\left[\aleph\cos\theta+\sin\theta\frac{\partial\ln w_s}{\partial s}-\frac{\mathrm{ctg}^2\beta}{r}-\frac{1}{2}\frac{\partial\mathrm{ctg}^2\beta}{\partial r}-\left(1+\mathrm{ctg}^2\beta\right)\frac{\partial\ln w_s}{\partial r}\right]-$$
$$-2\omega w_s\mathrm{ctg}\beta=T\frac{\partial S}{\partial r}-\frac{\partial H}{\partial r}+F_r+f_r. \qquad (2.24)$$

The projection of the equation of motion in the circumferential direction

Let us now consider the projection of the equation of motion (2.6) in the circumferential direction (2.14). Using (2.16), and the relationship between the coordinates *z*, *r* and *s*, *r* in the meridian plane

$$\frac{\partial}{\partial z}=\frac{1}{\cos\theta}\left(\frac{\partial}{\partial s}-\sin\theta\frac{\partial}{\partial r}\right),$$

equation (2.14) becomes:

- *for a given* $c_u r$ (inverse problem):

$$F_u = \frac{w_s}{r}\frac{\partial(c_u r)}{\partial s} - f_u; \tag{2.25}$$

- in the gap between vanes (free channel):

$$\frac{\partial(c_u r)}{\partial s} = 0; \tag{2.26}$$

- for a given β:

$$F_u = w_s^2\left[\frac{\sin\theta\,\mathrm{ctg}\,\beta}{r} + \frac{\partial \mathrm{ctg}\,\beta}{\partial s} + \frac{\partial \ln w_s}{\partial s}\mathrm{ctg}\,\beta\right] + 2\omega w_s \sin\theta - f_u. \tag{2.27}$$

These equations enable us to determine the projection of the blade force F_u in the circumferential direction. The radial component F_r is expressed through the circumferential according to (2.17).

The projections of the friction force on the coordinate axes

The expression for the friction force $\vec{f} = -\vec{W}\frac{T}{w^2}\left(\vec{W}, \nabla S\right)$ can be transformed by using the expression (2.16) and the binding ratio between the cylindrical coordinates *z*, *r* and the coordinates *s*, *r*:

$$\vec{f} = -\frac{\vec{W}}{w}\sin\beta T\frac{\partial S}{\partial s}, \tag{2.28}$$

whence we get the projection of the friction force on the coordinate axes:

$$f_r = -\sin^2\beta\sin\theta\, T\frac{\partial S}{\partial s}; \quad f_u = -\sin\beta\cos\beta\, T\frac{\partial S}{\partial s}.$$

The continuity equation is advisable to use in a form

$$d\psi = \frac{dG}{2\pi} = \chi r \rho w_s dn,$$

or, using the obvious relation $dn = dr\cos\theta$ (Fig. 2.3), we have:

$$\frac{\partial \psi}{\partial r} = r\rho w_s \cos\theta\, \chi. \tag{2.29}$$

If the working fluid can be considered as ideal gas, for which the equations of the state and of the process are simple expressions, using the equation [8] $i\sigma^{k-1}\rho^{1-k} = \text{const}$, we obtain

$$\frac{\partial i}{\partial s} = a^2\left(\frac{\partial \ln \rho}{\partial s} - \frac{\partial \ln \sigma}{\partial s}\right), \tag{2.30}$$

where $a^2 = (k-1)i = kRT$ – local sound velocity square.

Substituting (2.30) into (2.21), solving (2.21) and (2.20) as a system of linear equations with unknowns $\partial \ln w_s / \partial s$ and $\partial \ln \rho / \partial s$, we obtain for a given $c_u r$:

$$-\frac{\partial \ln w_s}{\partial s} = \frac{1}{1-\mathrm{M}_s^2}\left[\frac{\cos\theta}{r}\frac{\partial (r\,\mathrm{tg}\,\theta)}{\partial r} - \aleph\,\mathrm{tg}\,\theta + \right.$$
$$\left. + \frac{\partial \ln \chi}{\partial s} - \frac{c_u}{a^2}\frac{\partial c_u}{\partial s} + \frac{1}{a^2}\frac{\partial (uc_u)}{\partial s} + \frac{\partial \ln \sigma}{\partial s}\right]. \tag{2.31}$$

Note that

$$c_u \frac{\partial c_u}{\partial s} = \frac{c_u}{r}\frac{\partial (c_u r)}{\partial s} - \frac{c_u^2}{r}\sin\theta, \tag{2.32}$$

since $\partial r / \partial s = \sin\theta$, $\mathrm{M}_s = w_s / a$.

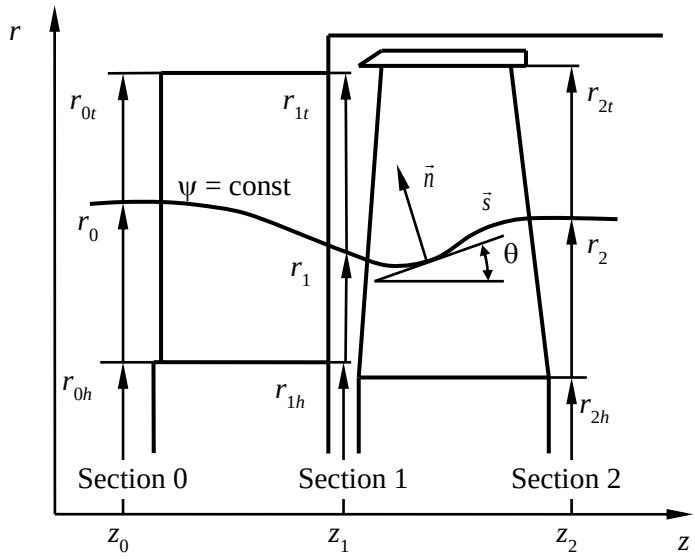

Figure 2.3 *Axial turbine stage meridian projection. Symbols used in the simplified stage calculation procedure.*

For a free channel from the projection of the equation of motion in the absolute coordinate system to the circumferential direction, obtain, that the circulation $c_u r = \text{const}$ along the meridian streamline and $\partial(c_u r)/\partial s = 0$.

Then *for a free channel* $(\chi = 1)$ from (2.31) we have:

$$-\frac{\partial \ln w_s}{\partial s} = \frac{1}{1-\mathrm{M}_s^2}\left[\frac{\cos\theta}{r}\frac{\partial(r\mathrm{tg}\theta)}{\partial r} - \aleph\mathrm{tg}\theta + \frac{(c_u r)^2}{a^2 r^3}\sin\theta + \frac{\partial \ln\sigma}{\partial s}\right]. \quad (2.33)$$

2.2.2 Aerodynamic Calculation of the Axial Turbine Stage in Gaps

The considered above in the general formulation, the problem of calculation of axisymmetric flows of a compressible fluid in the flow path of the axial turbine can be simplified and reduced to the calculation in gaps [9]. The flow in the axial gap is seen at the main proposals set out above. Within axial gap in the space free of the blades $\chi = 1$; because of its small length in the axial direction

the entropy S locally do not changes along the meridian streamlines (i.e. $\partial S/\partial s = 0$); it is possible to force components $F_r = f_r = 0$; stream keeps the direction of motion, telling him by blades (i.e., the angle of the flow β is set).

In these assumptions the radial equilibrium equation will differ from (2.24) in the absence of the right side of F_r and f_r:

$$w_s^2\left[\aleph\cos\theta+\sin\theta\frac{\partial\ln w_s}{\partial s}-\frac{\mathrm{ctg}^2\beta}{r}-\frac{1}{2}\frac{\partial\mathrm{ctg}^2\beta}{\partial r}-\left(1+\mathrm{ctg}^2\beta\right)\frac{\partial\ln w_s}{\partial r}\right]-$$
$$-2\omega w_s\mathrm{ctg}\beta-T\frac{\partial S}{\partial r}+\frac{\partial H}{\partial r}=0. \qquad (2.34)$$

From the energy equation (2.21), using (2.32), considering the fact that $\chi = 1$ and along the stream lines $\partial\left(c_u r\right)/\partial s = 0$ obtain

$$\frac{\partial\ln w_s}{\partial s}=\frac{1}{\left[1-w_s^2\left(\frac{\partial\rho}{\partial P}+\frac{\partial\ln\rho}{\partial i}\right)\right]}\left[\aleph\mathrm{tg}\theta-\frac{\cos\theta}{r}\frac{\partial\left(r\mathrm{tg}\theta\right)}{\partial r}-\right.$$
$$\left.-\frac{\left(c_u r\right)^2}{r^3}\sin\theta\left(\frac{\partial\rho}{\partial P}+\frac{\partial\ln\rho}{\partial i}\right)+T\frac{\partial S}{\partial s}\frac{\partial\rho}{\partial P}\right]. \qquad (2.35)$$

Radial equilibrium equation (2.34), written about the speed *w* (that gets rid of the derivative $\partial\mathrm{ctg}^2\beta/\partial r$) by going to the new independent variable ψ by a ratio

$$\frac{d}{dr}=r\rho w_s\cos\theta\frac{d}{d\psi},$$

takes the form

$$\frac{dw}{d\psi}=-\frac{\sin\beta}{r\rho\cos\theta}\left(B\sin\theta-\aleph\cos\theta+\frac{\mathrm{ctg}^2\beta}{r}+\frac{2\omega\mathrm{ctg}\beta}{w\sin\beta}\right)+$$

$$+\frac{1}{w}\left(\frac{dH}{d\psi}-T\frac{dS}{d\psi}\right). \tag{2.36}$$

The continuity equation can be represented as:

$$\frac{dr}{d\psi}=\frac{1}{r\rho w\sin\beta\cos\theta}. \tag{2.37}$$

Thus, flow in the gap of the turbine stage described by the system of two ordinary first order differential equations (2.36), (2.37) with the boundary conditions $r(0)=r_h$, $r(\psi^*)=r_t$.

The values $B=-\partial\ln W_S/\partial s$ are determined by (2.35), and the enthalpy – according to the equation energy

$$H=i+\frac{w^2}{2}-\frac{u^2}{2}=i+\frac{c^2}{2}-uc_u=\text{const}.$$

To calculate the temperature, density and entropy from the formulas (2.9) need to know other than the enthalpy *i* also pressure *P*, which for some *w* can be found from the second equation (2.8):

$$S_{in}=S_T\left(P, H+\frac{u^2}{2}-\frac{w^2}{2\psi^2}\right). \tag{2.38}$$

Consequently, the system of equations, describing the steam flow in the axial turbine stage gaps are as follows:

- after the guide vanes:

$$\left.\begin{aligned} \frac{dr_1}{d\psi} &= \frac{1}{r_1\rho_1 c_1 \sin\alpha_1 \cos\theta_1}; \\ \frac{dc_1}{d\psi} &= -\frac{\sin\alpha_1}{r_1\rho_1\cos\theta_1}\left(B_1\sin\theta_1 - \aleph_1\cos\theta_1 + \frac{\mathrm{ctg}^2\alpha_1}{r_1}\right) + \\ &+ \frac{1}{c_1}\left[\frac{di_0^*}{d\psi} + T_1\frac{dS_1}{d\psi}\right], \end{aligned}\right\} \tag{2.39}$$

where

$$B_1 = -\partial \ln w_{1s}/\partial s; \quad i_1 = i_0^* - c_1^2/2; \quad T_1 = T_1\left(i_1, P_1\right);$$

$$\rho_1 = \rho_1\left(i_1, P_1\right); \quad S_1 = S_1\left(i_1, P_1\right); \quad S_0^* = S_{1T}\left(P_1, i_0^* - c_1^2/\left(2\phi^2\right)\right).$$

Boundary conditions

$$r_1(0) = r_h; \; r\left(\psi^*\right) = r_s;$$

- after the rotor:

$$\left.\begin{aligned} \frac{dr_2}{d\psi} &= \frac{1}{r_2\rho_2 w_2 \sin\beta_2 \cos\theta_2}; \\ \frac{dw_2}{d\psi} &= -\frac{\sin\beta_2}{r_2\rho_2\cos\theta_2}\left(B_2\sin\theta_2 - \aleph_2\cos\theta_2 + \frac{\mathrm{ctg}^2\beta_2}{r_2} + \right. \\ &\left. + \frac{2\omega\,\mathrm{ctg}\,\beta_2}{w_2\sin\beta_2}\right) + \frac{1}{w_2}\left[\frac{di_0^*}{d\psi} - \frac{d\left(u_1 c_{1u}\right)}{d\psi} + T_2\frac{dS_2}{d\psi}\right], \end{aligned}\right\} \tag{2.40}$$

where

$$B_2 = -\partial \ln w_{2s}/\partial s; \quad i_2 = i_0^* - u_1 c_{1u} + u_2^2/2 - w_2^2/2; \quad T_2 = T_2\left(i_2, P_2\right);$$

$$\rho_2 = \rho_2\left(i_2, P_2\right); S_2 = S_2\left(i_2, P_2\right); S_1 = S_{2T}\left(P_2, i_{2w}^* - w_2^2/\left(2\psi^2\right)\right); i_{2w}^* = i_2 + w_2^2/2.$$

Boundary conditions:

$$r_2(0) = r_{2h};\ r_2(\psi^*) = r_{2t}.$$

The numerical realization of the stage thermal calculation problem

Mathematical models of axial turbine stages, discussed above, allow their calculation by setting some additional (closing) relations, for example, the distribution of the angles β and α (direct problem), the quantities $c_u r$, ρc_z, et al. (inverse problems).

To solve the direct problem of stage calculation in gaps the following information is required:

- form of the stage meridian contours, i.e. external and internal radii of axial sections;
- rotor speed ω;
- stagnation parameters at the stage input P_0^* and i_0^*;
- the geometrical characteristics of the blades: entry and exit angles, as well as blades count in the crowns, the chord, edge thickness and other parameters necessary for determining the velocity coefficients along the blade length;
- if the velocity coefficients are predefined – their distribution along the blade length.
- streamline slope angles θ and their curvature ℵ in fixed axial sections.

There are varieties of the direct problem with a given flow rate *G* and with a specified back pressure P_2. Solution of the problem with a fixed flow easier because the integration of the equations (2.39), (2.40) is made for a known $\psi^* = G/(2\pi)$ value and mathematically formulated as a two-point boundary value problem for a system of two ordinary first order differential equations of the form:

$$\left.\begin{aligned}\frac{dw}{d\psi} &= f_1(\psi, w, r);\\ \frac{dr}{d\psi} &= f_2(\psi, w, r),\end{aligned}\right\} \tag{2.41}$$

with boundary values: $r(0) = r_h$; $r(\psi^*) = r_t$.

Right sides of equation (2.41) are calculated according to the formula of the system of equations (2.39), (2.40).

The decision imposed positivity of w (unseparated flow condition).

From physical considerations it is known that problem (2.41) can have either two solutions, corresponding sub- and supersonic flow mode, either one or do not have a solution.

One way of solving the problem (2.41) is to reduce it to finding the root of the transcendental equation, which serves for the selection of the missing boundary condition at the hub $w(0) = w_h$. Indeed, setting a boundary condition w_h and integrating (2.41) as the Cauchy problem with the initial conditions $r(0) = r_h$; $w(0) = w_h$, we obtain at ψ^* an approximate value of the outer radius $r(\psi^*) = \tilde{r}_t$. Considering $\tilde{r}_t$ as a function w_h we obtain the equation with one unknown w_h:

$$\tilde{r}(w_h) - r_t = 0. \tag{2.42}$$

Thus, for the solution of the direct problem of the stage calculation with a given flow rate is required to solve the system of transcendental equations:

$$\left.\begin{aligned}&\tilde{r}_{1t}(c_{1h}) = r_{1t},\\ &\tilde{r}_{2t}(c_{1h}, w_{2h}) = r_{2t}.\end{aligned}\right\}. \tag{2.43}$$

The solution of (2.43) is made in two stages: first, the first equation is solved and the distribution of the flow in fixed axial gap is found, then, knowing the parameters entering the impeller can solve the second equation. That is, the problem is reduced to determining the roots of the equation with one unknown for each of the two equations (2.43). For the calculation of the subsonic solutions of (2.43) can be successfully used the methods of nonlinear programming. The system (2.43) is solved by sequential minimization of residuals

$$\left.\begin{aligned} \Delta_1^2 &= \left[\tilde{r}_{1t}\left(c_{1h}\right) - r_{1t}\right]^2, \\ \Delta_2^2 &= \left[\tilde{r}_{2t}\left(w_{2h}\right) - r_{2t}\right]^2. \end{aligned}\right\} \tag{2.44}$$

using one of the described one-dimensional extremum search methods.

Solution of the problem with a given back pressure P_2 (flow rate unknown) is more complicated. To determine the unknown mass flow G to the system of equations (2.43) is necessary to add one more thing – a limit on the heat drop.

In this formulation of the problem it seems appropriate to set the mass flow averaged pressure according to the formula

$$\int_0^{\psi^*} P_2 d\psi = \psi^* P_{2m.def.}. \tag{2.45}$$

In view of (2.45) to calculate the level with a given back pressure is needed to solve a system of three equations with three unknowns:

$$\left.\begin{aligned} \Delta_0 &= h\left(c_{1h}, w_{2h}, \psi^*\right) - h_0 = 0; \\ \Delta_1 &= \tilde{r}_1\left(c_{1h}, \psi^*\right) - r_{1t} = 0; \\ \Delta_2 &= \tilde{r}_2\left(c_{1h}, w_{2h}, \psi^*\right) - r_{2t} = 0. \end{aligned}\right\} \tag{2.46}$$

Numerically, the problem is solved to minimize the sum of squared residuals

$$I^* = \Delta_0^2 + \Delta_1^2 + \Delta_2^2 \tag{2.47}$$

on three variables c_{1h}, w_{2h}, ψ^* using one of the multidimensional extremum search methods.

A maked up mathematical model describing the flow in the axial gaps of turbomachine (equation (2.39), (2.40)), allows the calculation of supersonic flow (including the transition through the speed of sound), which $M_s < 1$, i.e., in the case of the meridional component of velocity less than the velocity of sound. Specified the conditions satisfy all existing stages of powerful steam turbines.

Calculation of supersonic stages must be performed with a given back pressure, because otherwise does not provide a unique solution of the equation of the form (2.41). At the same time, the system of transcendental equations (2.46) in the variables c_{1h}, w_{2h}, ψ^* in contrast to (2.43) has a unique root.

Another feature of the supersonic stages calculation is the need to consider the flow deflection in an oblique cut at Mach numbers higher than unity. For this purpose it is possible to use a method of determining the flow deflection angle in an oblique cut comprising in equating flow rate into the throat section and behind the blade [10, 11].

In this case, to calculate the residuals of equations (2.44), (2.46) it is necessary to integrate the system of ordinary differential equations of the form (2.41), namely (2.39), (2.40). These equations are due to the complexity of the form of the right sides in the general case can be integrated numerically. When integrating (2.39) (2.40) should be borne in mind that at each step of pressure shall be determined by solving the equations of the form (2.38), which greatly complicates the task.

Finally, we note that because of the existence of the right sides of (2.38), (2.40), a member $T\partial S/\partial\psi$, the system, generally speaking, can not be considered as written in the form of Cauchy, as these non-linear supplements are some of the functions w_2 or c_1, r and their derivatives. When integrating these terms are determined by successive approximations.

The important point is the choice of numerical methods for integrating systems of the form (2.41). Extensive experience in solving such problems suggests the possibility of partitioning the integration interval to a small number of steps (5–10). As a result of numerical experiments comparing different methods, preference was given to the modified Euler's method [12], which has the second order of accuracy for the integration step.

The leakage calculation is necessary to conduct together with a stage spatial calculation, the results of which are determined the parameters along a height in the calculation sections, including the meridian boundaries of the flow part.

The stage capacity depends on the value of clearance (or leakages), in connection with which calculation of the main stream flow is made by mass flow amplification at fixed the initial parameters and counter-pressure on the mean radius, or with counter-pressure elaboration at fixed initial parameters and mass flow.

The need for multiple steps in optimization problems requires a less labor-capacious, but well reflecting the true picture of the flow, methods of axisymmetric stage calculation. Its main point is to calculate the stage parameters in the axial gaps supplemented by the algorithm of stream lines slope and curvature refinement in the design sections.

When calculating the stage taking into account leakage, the continuity equation is convenient to take the form:

$$\frac{\partial \psi}{\partial r} = \mu r \rho w_s \cos\theta\,, \tag{2.48}$$

where μ – mass transfer coefficient, which allows to take into account changes in the amount of fluid passing through the crowns, and at the same time to solve a system of ordinary differential equations in sections in front of and behind the impeller like a constant mass flow rate.

As shown, the calculation of spatial flow in the stage with the known in some approximation the shape of the stream lines is reduced to the solution in the sections $z_1 = \text{const}$ and $z_2 = \text{const}$ (Fig. 2.3) of a system of ordinary differential equations (2.39) and (2.40), where as independent variable a stream function ψ is taken. Thus, the equations describing the flow in the axial gap, presented in the form of:

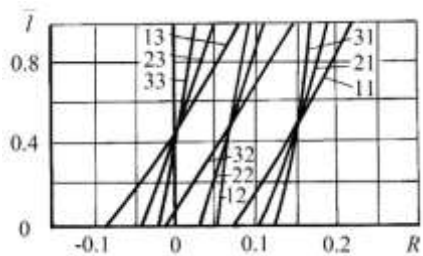

Figure 2.4 *Estimated distribution of the reaction degree in a series of stages with* $D_m/l = 19$ *[13].*

- in the section after the guide vanes:

$$\left.\begin{aligned} \frac{dr_1}{d\psi} &= f_{11}(\psi, r_1, c_1); \\ \frac{dc_1}{d\psi} &= f_{12}(\psi, r_1, c_1); \\ r_1(0) &= r_{1h}; \quad r_1(\psi^*) = r_{1t}; \end{aligned}\right\} \tag{2.49}$$

- in the section after rotor:

$$\left.\begin{aligned} &\frac{dr_2}{d\psi} = f_{21}\left(\psi, r_1, c_1, r_2, w_2\right); \\ &\frac{dw_2}{d\psi} = f_{22}\left(\psi, r_1, c_1, r_2, w_2\right); \\ &r_2\left(0\right) = r_{2h}; \quad r_2\left(\psi^*\right) = r_{2t}. \end{aligned}\right\} \tag{2.50}$$

The solution of the boundary problems (2.49), (2.50) for a given mass flow rate is reduced to finding the roots of the two independent transcendental equations (2.43) with respect to the hub velocities c_{1h}, w_{2h}.

For a given backpressure to the number of defined values the mass flow ψ^* is added and the problem reduces to solving a system of three equations. As a third equation the stage heat drop constraint is added (2.45) that can be symbolically written as

$$h\left(c_{1h}, w_{2h}, \psi^*\right) - h_0 = 0.$$

Systems of equations are solved using the methods of nonlinear programming.

An approximate method of meridian stream lines form amplification using their coordinates in the three sections, is to construct an interpolation cubic spline at a given slopes at the flow path boundaries. In order to accelerate the convergence the stream line curvature is specified with lower relaxation. Previous calculations showed that the interpolation process converges with sufficient accuracy in 3…5 iterations.

Mass flow rates through crowns carried out in parallel with the streamlines construction. The algorithm allows to solve the direct problem of the spatial stage calculation in the gaps in various statements, with given or variable in the process

of calculating the streamlines, velocity and flow coefficients of crowns, at various ways of flow angles distribution along the height, for a perfect gas or steam.

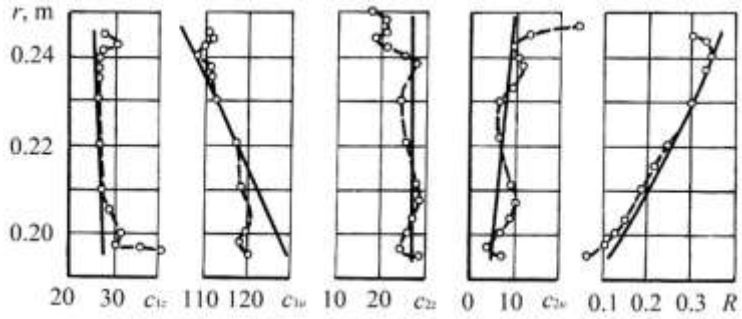

Figure 2.5 *Estimated (——) and experimental (---- o ----) distribution of parameters in the M1 stage gaps* $D_m/l = 8.3$ *[13].*

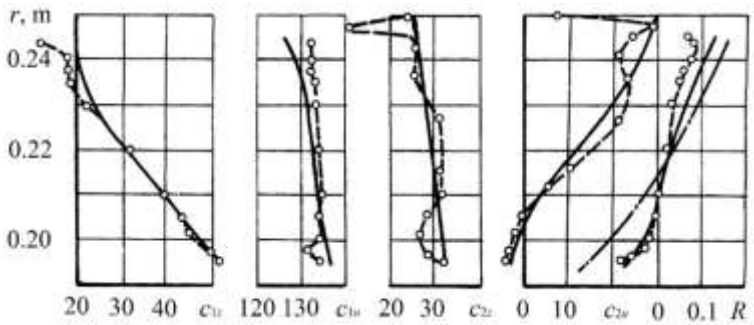

Figure 2.6 *Estimated (——) and experimental (---- o ----) distribution of parameters in the P3 stage gaps* $D_m/l = 8.3$ *[13]: —• ——calculation of cylindrical theory.*

The algorithm was tested by comparing the calculation results with the exact solutions, as well as with the experimental data obtained for a large number of stages of the experimental air turbines in the turbine department of NTU "KhPI" [13–14, 15]. The results of calculations and experiments illustrated in Fig. 2.4–2.12. It should be stated a good calculations agreement with the experimental result for the various stages of the different elongation, meridian shape contours, twist laws and the reaction degree at the mean radius.

The greatest difficulty to calculate present stages with the steep opening of the flow path (Fig. 2.12), and the cylindrical stages with inversely twisted guide vanes (Fig. 2.4, 2.6–2.8).

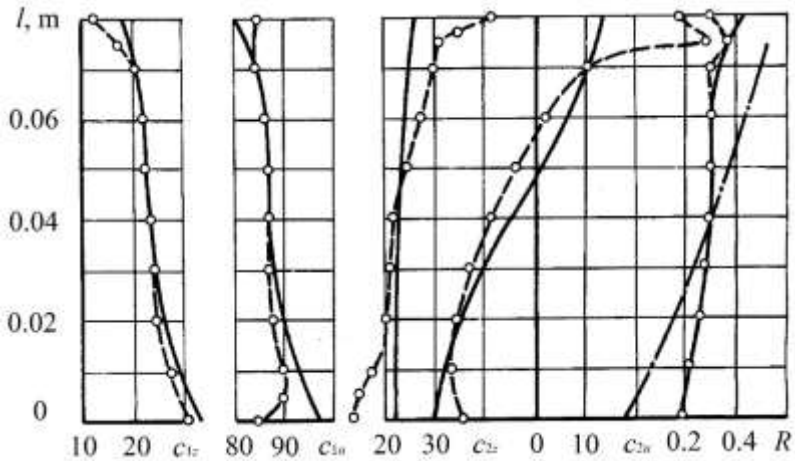

Figure 2.7 *Estimated (——) and experimental (---- o ----) distribution of parameters in the stage 41 gaps with* $D_m/l = 5.13$ *[13]; —• —– calculation of cylindrical theory.*

The calculation of stages with inverse twist using the proposed method allows to obtain a valid gradient of reaction degree and circumferential velocity component of the stage, while the calculation provided in assumption of cylindrical flow gives results that differ significantly from the experimental data (Fig. 2.6–2.8). The technique allows to take into account also the effect of the law of the impeller's twist on the distribution of parameters in the gap between guide vane and rotor. This is evidenced by the comparison stages 41 and 42 (Fig. 2.7, 2.8) with the same nozzle unit, the first of which has a cylindrical impeller, and the second – twisted by constant circulation law.

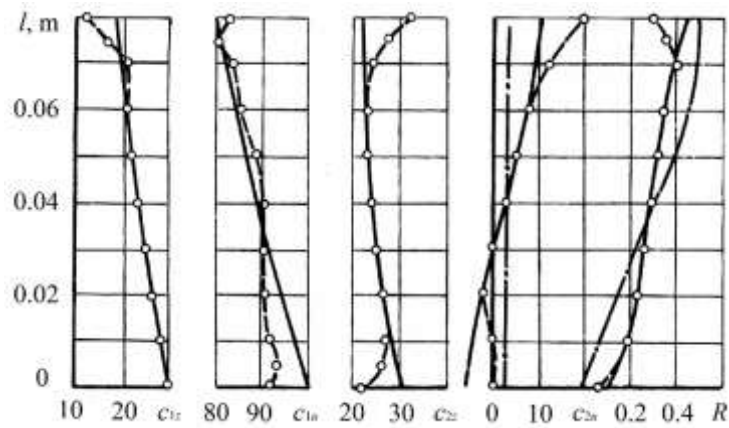

Figure 2.8 *Estimated (——) and experimental (---- o ----) distribution of parameters in the stage 42 gaps* $D_m/l = 5.13$ *[13]; —• —– calculation of cylindrical theory.*

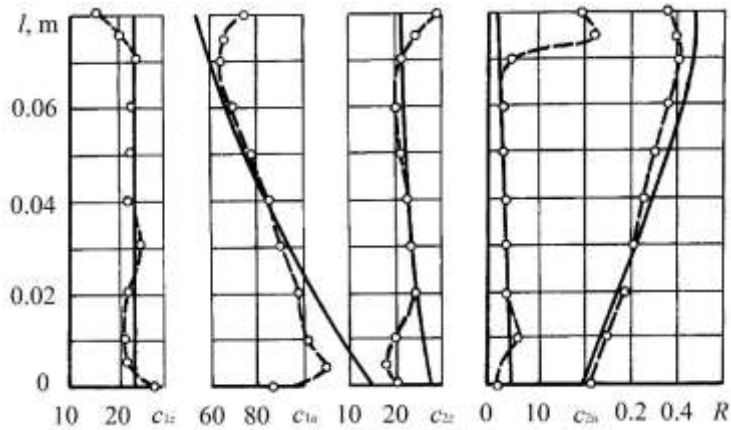

Figure 2.9 *Estimated (——) and experimental (---- o ----) distribution of parameters in the stage 32 gaps* $D_m/l = 5.13$ *[13].*

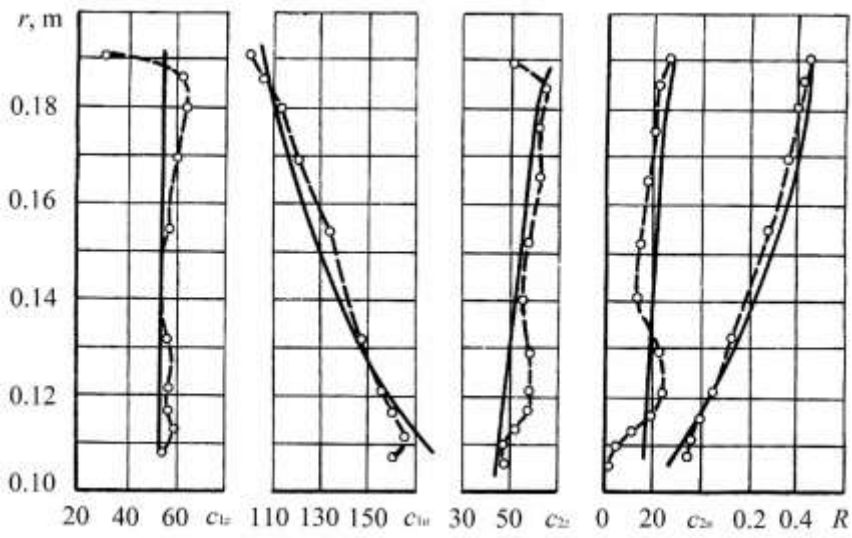

Figure 2.10 *Estimated (——) and experimental (---- o ----) distribution of parameters in the stage I gaps* $D_m/l = 3.6$ *(the author's tests).*

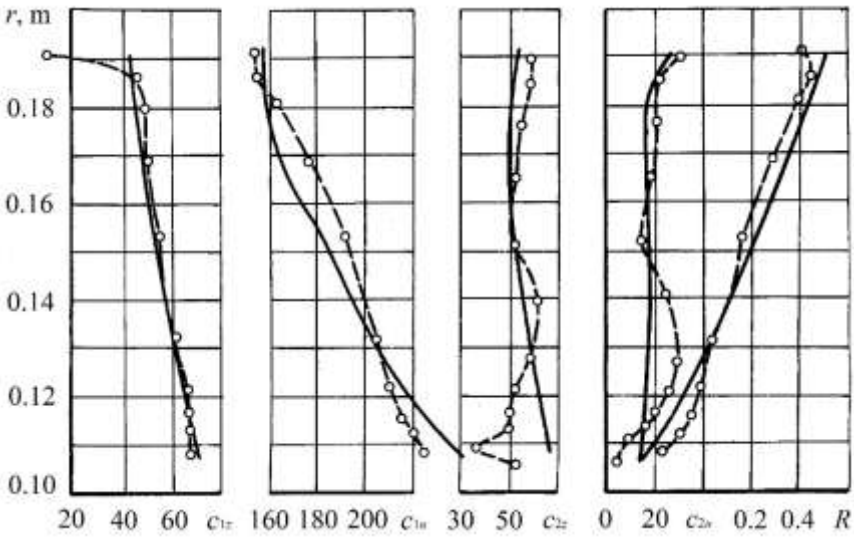

Figure 2.11 *Estimated (——) and experimental (---- o ----) distribution of parameters in the stage gaps II* $D_m/l = 3.6$ *(the author's tests).*

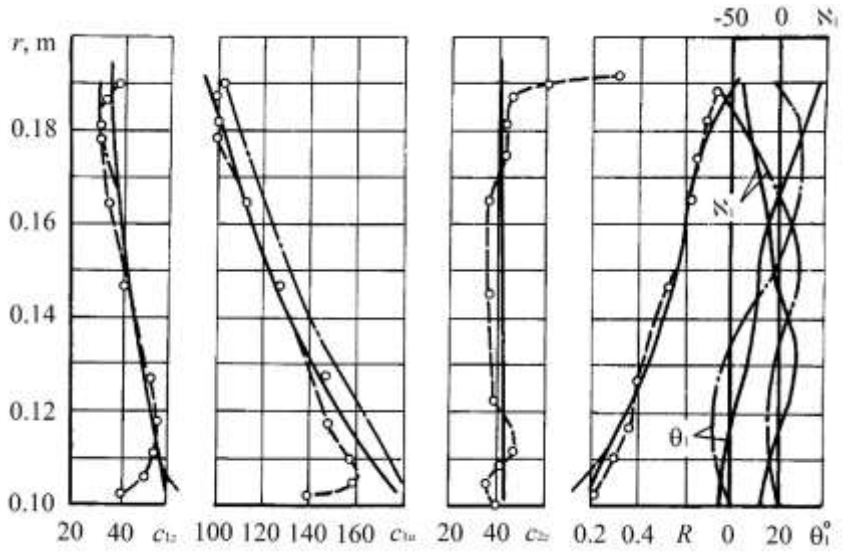

Figure 2.12 *Estimated (——) and experimental (---- o ----) distribution of parameters in the stage 33 gaps* $D_m/l = 3.2$ *[13]; —• —– full axisymmetric statement calculation.*

2.2.3 Off-Design Calculation of Multi-Stage Steam Turbine Flow Path

Formulation of the problem

The off-design analysis problem is to determine the gas-dynamic characteristics derived from the design calculation such as the size of the flow path (FP) and the parameters that determine the long-term (steady) operation of the turbine. The need to analyze FP off-design modes arises when assessing aero- and thermodynamic, power, strength parameters of the turbine in extreme operating conditions, the choice of method for control and calculation of steam distribution, for turbines designed to operate at changing the regime parameters (speed, unregulated steam extraction and so on).

The specifics of these problems requires a gas-dynamic calculations in a direct statement, which is more labor intensive than the calculations commonly

used in the design stage. In connection with this methods designed for use with a computer optimization procedures must meet several requirements:

- to base on the equations of motion of a real working fluid in the flow path of the multi-stage turbine;
- to consider with the required accuracy the influence of geometrical and operational parameters on the loss factors of the FP elements;
- to allow to conduct calculations with varying from section to section the mass flow rates;
- to be highly reliable and economical in terms of consumption of computer resources, i.e. make it possible to carry out multi-variant and optimization calculations.

To calculate high, medium and, to a lesser extent, the low-pressure parts of powerful steam turbines, justified the use of one-dimensional gas dynamics calculations using the simplified radial equilibrium equations in a axial clearance, the leaks balance at the root of the diaphragm design stages and the calculation method of the FP moisture separation. Accounting for the loss of kinetic energy and efficiency assessment should be carried out by successive approximations based on the current results of the gas-dynamic calculation and empirical relationships, and reliability of the results – achieved by comparison with experimental results and the introduction of necessary adjustments.

Should be regarded as a satisfactory the accuracy of coincidence of calculated and experimental values of the relative losses in the range of 5…7% for FP made with straight or twisted by constant circulation law blading in the absence of the sharp curvature of the meridian contours. When the actual loss levels of 10...30% error in determining the efficiency, thus lies in the range of 0.5...2% [15].

Method of calculation

One-dimensional steady-state equilibrium adiabatic motion of water vapor in the flow path in a coordinate system rotating with angular velocity ω, sought a system of equations:

- energy

$$H = i + \frac{w^2 - u^2}{2}; \tag{2.51}$$

- continuity

$$G = F\rho w_z; \tag{2.52}$$

- process

$$S_0 - S\left(P, \frac{1}{\psi^2}\left[i - \left(1 - \psi^2\right) i_w^*\right]\right) = 0; \tag{2.53}$$

- state

$$T = T(P, i);\ \rho = \rho(p, i);\ S = S(p, i);\ P = P(i, S);\ i = i(P, S); \tag{2.54}$$

- flow kinematic parameters relations.

The solution to this system of equations for an isolated axial turbine stage in a direct statement requires:

- stage input enthalpy i_0^*;
- stage output pressure P_{2def};
- angular rotational speed ω;
- mean diameters of sections D_{1m}, D_{2m} and blade lengths l_1, l_2;
- cascade's output effective angles α_{1e}, β_{2e};

- data to estimate blades velocity factors: chords, number of blades, edge thickness, geometry entry angles so on;
- the data for the calculation of additional energy losses, such as the types of seals and their sizes, the values of axial and radial clearances, the number of bonding wires, etc.

The two main statements involve mass flow G_0 determination at certain stagnated pressure P_0^* at stage inlet, or the P_0^* definition at known flow rate. It is also possible the solution of the problem with given at the same time G_0 and P_0^* changing angles α_{1e} or β_{2e}, in particular, makes it possible to simulate the nozzle assembly with rotary blades. In all cases, subject to the definition of the flow speed c_1 and w_2.

For definiteness we shall consider the problem with fixed P_0^* and mass flow determination. We transform the equation of continuity (2.52) for the nozzle in view of (2.51), (2.53), (2.54):

$$G = \rho_1 \left(P\left(i_0^* - \frac{c_1^2}{2\phi^2}, S_0^*\left(P_0^*, i_0^*\right)\right), i_0^* - \frac{c_1^2}{2}\right) c_1 \sin\alpha_1 F_1 \tag{2.55}$$

with unknown c_1 and G.

Similarly, after the impeller

$$G = \rho_2 \left(P\left(H + \frac{u_2^2}{2} - \frac{w_2^2}{2\psi^2}, S\left(P_1, i_1\right)\right), H + \frac{u_2^2}{2} - \frac{w_2^2}{2}\right) w_2 \sin\beta_2 F_2, \tag{2.56}$$

where

$$H = i + \frac{c_1^2}{2} - u_1 c_{1u};\ P_1 = P\left(i_0^* - \frac{c_1^2}{2\phi^2}, S_0^*\right);\ i_1 = i_0^* - \frac{c_1^2}{2}.$$

This equation contains the unknown c_1, G, w_2.

Under α_1 and β_2 at subsonic flow understood the cascade's effective angles, and at supersonic – flow angles in the oblique cut-off by the Ber formula.

The third equation is:

$$P\left(H+\frac{u_2^2}{2}-\frac{w_2^2}{2\psi^2}, S\left(P_1, i_1\right)\right)=P_{2def}. \tag{2.57}$$

Under certain velocity factors φ and ψ to determine the unknown c_1, G, w_2, there are three equations (2.55)–(2.57), which in general terms be written as follows:

$$\left.\begin{aligned} &g_1\left(G, c_1\right)=0;\\ &g_2\left(G, c_1, w_2\right)=0;\\ &h\left(G, c_1, w_2\right)=0. \end{aligned}\right\} \tag{2.58}$$

The system (2.58) is solved numerically by minimizing the sum of squared residuals $g_1^2+g_2^2+h^2$ using the conjugate gradient method.

Calculation of multistage flow path does not differ systematically from the stage calculation. An equation of (2.58) is written for each of the stages, which leads to a system of the form

$$\left.\begin{aligned} &g_{1j}\left(G, c_{1j}, c_{1j-1}, \ldots, w_{2j-1}, w_{2j-2}, \ldots.\right)=0;\\ &g_{2j}\left(G, c_{1j}, c_{1j-1}, \ldots, w_{2j}, w_{2j-1}, \ldots.\right)=0,\ j=1, \ldots, n;\\ &h\left(G, c_{1n}, \ldots, c_{11}, w_{2n}, \ldots,\ w_{21}\right)=0, \end{aligned}\right\} \tag{2.59}$$

where j – stage index; n – number of stages in the FP.

The numerical solution is carried out by minimizing the function

$$\sum_{j=1}^{n}\left(g_{1j}^2+g_{2j}^2\right)+h^2$$

by $2n+1$ unknowns $c_{1j}, w_{2j}, (j=1,\ldots,n), G$.

Sections may have different mass flows because of the leaks, district heating or regenerative steam extraction, moisture separation and so on. In the equations (2.59) in this case instead of a mass flow rate *G* in the relevant sections should take the current value

$$G_k = G_{k-1} + \Delta G_k,$$

where ΔG_k – given or confirmed in iterations the mass flow change in the transition from $(k-1)$ section to the *k*-th $(k=1\ldots2n)$.

The unknown is considered the G_0 mass flow at the FP entrance.

After the solution of (2.58) or (2.59) all the parameters of the flow calculated, loss factors and the actual mass flows in sections adjusted. The required number of iterations is usually equal to 3...4.

Kinetic energy loss determination

Losses associated with the leakage of the working fluid are considered separately. The remaining components are divided into losses in cascade and auxiliary, which are allocable to the stage heat drop.

Methods of assessing the losses in cascades based on research [8, 16] with a corresponding adjustment of empirical dependencies using test data about profiles used in the turbine building [17, 18].

Following [16], the loss factor in the cascade $X=\left(1-\psi^2\right)/\psi^2$ is the sum of the factors of profile X_p and secondary X_s losses, which are defined as follows:

$$X_p = X_{pb} N_{\mathrm{Re}} N_i N_{iy} N_t + \Delta x_t + \Delta x_{\mathrm{M}} + \Delta x_y , \tag{2.60}$$

where X_{pb} – base profile loss; N_{Re} – Reynolds number correction; N_i – incidence angle correction; N_{iy} – correction for the angle of attack associated with the elongation of the leading edge profile; $N_t, \Delta x_t$ – trailing edge thickness corrections; Δx_{M} – Mach number correction at $\mathrm{M} > 1$; Δx_y – correction due to the elongation of the input portion of the profile with a zero angle of attack.

$$X_s = X_{sb} N_{\mathrm{Re}} N_{b/l} N_\delta , \tag{2.61}$$

where X_{sb} – base secondary loss; $N_{b/l}$ – relative blade height correction; N_δ – an amendment to the length of hanging visor.

Corrections for the Reynolds number, angle of attack, the thickness of the trailing edge, at supersonic flow are taken over without change [19]. The amendment to the angle of attack in the profiles provided with an extension of the leading edge, is estimated according to experimental studies on the standard nozzle profiles and the impact of the extension on the profile loss – NPO CKTI the procedure [20].

The basic component of the profile X_{pb} obtained by a corresponding adjustment to the loss level of graphic dependence [16]. Basic secondary loss is determined by the corrected chart [16], an amendment to the ratio of the chord to the height of the blade $N_{b/l}$ – according to [16], and the coefficient N_δ taking into account the length of the visor hanging over the trailing edge of the blade – based on experimental data on nozzle standard profiles test data.

When assessing the energy losses in the rotor blades, can be taken into account the effect of the periodic incident flow unsteadiness caused by the

presence of traces of the previous nozzle cascade, as amended N_γ. The degree of non-uniformity of the incoming flow is taken over [8].

Additional energy losses are the disc friction and ventilation, extortion, humidity, the presence of the wire bonding and friction in the open and closed axial clearance in accordance with the guidelines [21].

Leak sand leakage losses calculation

It is estimated that losses caused by leakage of the working fluid into the gaps of the flow path, associated with a decrease in the mass flow rate through the crowns, aerodynamic and thermodynamic mixing with the main flow losses, as well as the deviation of the kinematic parameters in the gaps comparing to the design.

To determine the thermodynamic parameters near the flow path margins, needed to calculate the leaks mass flows, a simplified equation of radial equilibrium $\partial P = \frac{\rho c_u^2}{r}\partial r$ is involved. In the gap between vanes considered that $c_u r = \text{const}$, $\rho_1 = \text{const}$, and behind the stage $c_{2u} = \text{const}$, $\rho_2 = \text{const}$.

Leaks in the root area of multistage flow paths are the solution of the mass flow balance equations through diaphragm, root seals and discharge holes taking into account given dependences of the gaps flow factors and friction coefficients of the regime and geometrical parameters, changes in pressure and flow swirling in the disk chambers along the radius at the presence of the working fluid flow etc.

Evaluation of leakages based on a calculation of the anterior chamber only, first, does not allow correct balance the mass flows along the FP, and secondly, may lead to considerable errors as the leakage values and axial forces, particularly at the off-design operation.

The algorithm is developed for the calculation of leakages in multistage FP, in which can be built leaks circuit within the cylinder based on the majority of the factors, influencing them [14]. Calculation of mixing the main flow with leaks through tip and root gaps is based on the balance equations for flow, enthalpy, and entropy. Raising the equations of motion for the evaluation of aerodynamic mixing losses allows, under certain assumptions, take into account the impact on the mixing loss of the blowing working fluid angle.

The third group of losses factors, caused by leaks, mainly, through a change of velocity coefficient of cascades after gaps, where mixing occurs, due to variations of inlet flow angles.

2.2.4 Simulation of Axisymmetric Flow in a Multi-Stage Axial Turbine

To solve this problem, we used a combined one-dimensional and axisymmetric approach.

A mathematical model of a coaxial flow of the working fluid in the flow part of a multi-stage axial turbine

This model belongs to the class of quasi- two-dimensional models, and is a logical continuation of the one-dimensional model of the FP shown in subsection (2.2.3). All equations, methods and techniques of assessment of energy dissipation in the elements of FP used in the one-dimensional model, have been fully utilized in the development of quasi- two-dimensional model of the coaxial FP.

A distinctive feature of the coaxial model is the fact that the system of equations (2.59) are determined not to cross-sections corresponding to the mean radius of the multistage FP crowns, and for each current streams along its midline.

The system of equations (2.59) in a coaxial FP model in a general form as follows:

$$\begin{cases} g_{1(i,\,j)}\left(G, c_{1(i,\,j)}\right)=0; \quad g_{2(i,\,j)}\left(G, c_{1(i,\,j)}, w_{2(i,\,j)}\right)=0; \quad (i=1); \\ g_{1(i,\,j)}\left(G, c_{1(i,\,j)}, w_{2(i-1,\,j)}\right)=0; \quad g_{2(i,\,j)}\left(G, c_{1(i,\,j)}, w_{2(i,\,j)}\right)=0; \quad (i=2); \\ \ldots\ldots\ldots\ldots\ldots\ldots\ldots\ldots\ldots\ldots\ldots\ldots\ldots\ldots\ldots\ldots\ldots\ldots \\ g_{1(n,\,m)}\left(G, c_{1(n,\,m)}, w_{2(n-1,\,m)}\right)=0; \quad (i=n); \\ g_{2(n,\,m)}\left(G, c_{1(n,\,m)}, w_{2(n,\,m)}\right)=0; \quad (i=n); \\ (i=1,\ldots,n); \\ h\left(G, c_{1(n,\,j)}, c_{1(n-1,\,j)}, \ldots, c_{1(1,\,j)}, w_{2(n,\,j)}, w_{2(n-1,\,j)}, \ldots, w_{2(1,\,j)}\right)=0; \\ (j=1,\ldots,m), \end{cases} \tag{2.62}$$

where m – is equal to increased by two the number given sections (streamlines) along the radius of the blades; j – number of cross-section along the blade height (the first cross section is located at the root level).

Accordingly, the dimension of the system of equations in a mathematical model of a coaxial flow in the FP is equal to $(n + 1)m$.

The marked increase in the number of sections required for a significant approaching of the root and near-the-tip stream lines to the root level and the peripheral area, respectively. With the same purpose the cross sectional area of the extreme stream lines assigned minimum values (1% of area of the corresponding vane). For the first iteration the remaining cross-sectional areas between the stream lines are equal and are determined as follows:

$$S_{(k,\,j)}=0.98S_{(k)}(m-2),$$

where $S_{(k)}$ – cross-section area of k-th vane.

After determining the $S_{(k,\,j)}$ are determined the radii of mean lines of all flow streams, angular velocities and the values of all the geometric characteristics of the cascades at those radii. In subsequent iterations, the average radius of the stream lines, and all the characteristics of cascades and the working flow determined in accordance with the obtained distribution of the mass flow the radius of corresponding vanes. This ensures the equality of the working fluid (including the extractions and leakages) along the respective stream lines.

Considering that the system of equations (2.62) is based on the one-dimensional flow theory for each stream line, where there is no equation of radial equilibrium, it becomes apparent that the above-described method of stream tubes sizing, is most accurate by using this model, it will be possible to evaluate the characteristics of the axial turbines, which vane's twist corresponds to the $c_u r = \text{const}$ law, or close to it. For practical tasks coaxial mathematical model is most suitable when assessing the characteristics of the high pressure cylinder (HPC) flow path.

Despite the fact that the flow of working fluid along each stream tube in consideration of coaxial mathematical model of the FP is modeled in accordance with the one-dimensional theory, when calculating the flow kinematics the slope angles of each stream line are taken into account (curvature of the streamlines is not considered) and identifies all components of the flow velocity in axial gaps. To determine the angles of the middle line of the stream tubes cubic spline interpolation is used. A well-known feature of these splines is the coincidence of the first and second derivatives of the neighboring areas in the nodes of the spline coupling. It allows us to describe the midline of a stream line using dependence, which provides its most smooth shape.

Because in the outer iteration loop of the multistage axial turbine FP coaxial mathematical model (as well as in the one-dimensional mathematical model of

the FP), the quantities of moisture separation, tip leakage and near-the-hub leakages and the working fluid extractions to the heating system and feed-water heating refer to the entire stage, and not to each stream tube, the question of adequate distribution of the marked mass flow changes between the stream tubes arise.

In this case, there are two variants of distribution of leaks and the working fluid extractions between the stream tubes:

1) The total change in the mass flow of the working fluid in the transition from one vane to another distributed between streams in proportion to their cross-section areas (1-st iteration).

2) The distribution of mass flow changes in proportion to the stream tube mass flow, the size of which is determined from the condition that the mass flow of each stream tube in accordance with the law of the flow rate changing along the radius of the stage, obtained in the previous iteration.

Additionally, there are also two versions of the distribution of secondary loss of height of the blade:

1) The secondary losses are concentrated at the ends of the blades.

2) The secondary losses are evenly distributed among all streams tubes (proportional to the mass stream tube mass flow).

Integral indicators of each stage in the coaxial model are determined by the relationships below

$$\begin{cases} G_{0(i)} = \sum_{j=1}^{m} g_{0(i,\,j)}; \quad G_{1(i)} = \sum_{j=1}^{m} g_{1(i,\,j)}; \quad G_{2(i)} = \sum_{j=1}^{m} g_{2(i,\,j)}; \\ N_{st(i)} = \sum_{j=1}^{m} N_{str(i,\,j)}; \quad N_{(i)} = \left(\sum_{j=1}^{m} g_{1(i,\,j)} \cdot h_{(i,\,j)} \right) \Big/ G_{1(i)}; \\ \eta_{(i)} = \left(\sum_{j=1}^{m} g_{0(i,\,j)} \cdot \eta_{(i,\,j)} \right) \Big/ G_{0(i)}; \quad Lu_{(i)} = \left(\sum_{j=1}^{m} g_{0(i,\,j)} \cdot lu_{(i,\,j)} \right) \Big/ G_{0(i)}; \\ \Phi^2_{(i)} = \left(\sum_{j=1}^{m} g_{1(i,\,j)} \cdot \phi^2_{(i,\,j)} \right) \Big/ G_{1(i)}; \quad \psi^2_{(i)} = \left(\sum_{j=1}^{m} g_{2(i,\,j)} \cdot \psi^2_{(i,\,j)} \right) \Big/ G_{2(i)}, \end{cases} \tag{2.63}$$

where $g_{0(i,\,j)}, g_{1(i,\,j)}$ and $g_{2(i,\,j)}$ – working fluid mass flows of the *j*-th stream tube entering the *i*-th stage and through its nozzle and working cascade, respectively; $N_{str(i,\,j)}, h_{(i,\,j)}, lu_{(i,\,j)}$ – power, heat drop and disposable work of the *j*-th stream tube of *i*-th stage; $\eta_{(i,\,j)}, \phi^2_{(i,\,j)}, \psi^2_{(i,\,j)}$ – the efficiency, the velocity coefficients squares of the nozzle and working cascades along the *j*-th stream tube of the *i*-th stage. Similarly other integral indicators of the axial turbine FP stages are determined.

A mathematical model of an axisymmetric flow of the real working fluid in a multi-stage axial turbine FP

Despite the fact that the coaxial mathematical model of the flow of the working fluid in the FP, as described in the previous section, has a fairly narrow range of independent use, yet it has a sufficiently high potential. If the formation of the transverse dimensions of the stream tubes to carry the light of the decision of the radial equilibrium equation (sections 2.2.1, 2.2.2), this model can be successfully used in the calculation of axisymmetric flow in a multi-stage axial turbine FP with virtually any kind of its crowns twists.

The use of coaxial FP model to evaluate the distribution of the static pressure behind the rotor blades to determine disposable heat drops of each stage that you

need to solve the axisymmetric problem "with a given back pressure". It is known that only in such a setting is possible to find the correct solution to supersonic stages. Marked problems for each crown of multi-stage flow path solved by the means of stream line curvature method. Thus, in view of (2.46) and the system of equations (2.62), the scheme for solving the problem "with a specified back pressure" for a multi-stage axial flow turbine parts will be as follows:

- Using a coaxial FP model made an initial assessment of the static pressure distribution along the radius of the stages working crowns.
- Relations obtained according to the static pressure of the stages as the boundary conditions are transferred to the axisymmetric simulation unit (sections 2.2.1, 2.2.2).
- As a result of solution of the boundary value problems (2.49) and (2.50), for each stage the distributions of the mass flow of the working fluid along the nozzle and working crowns radii for all FP stages are formed.
- The resulting distributions of the mass flow of the working fluid along the radii of the crowns are used to determine the average of the radii of new stream tubes and areas of cross-sections for the coaxial FP model.
- Calculation of coaxial FP model with the new values of the transverse dimensions of the stream tubes is performed.

For clarity, the above-described sequence of solving axisymmetric problem "with a given back pressure" for multi-stage FP is shown in Fig. 2.13.

Consider some features of the numerical solution of axisymmetric problem for multi-stage FP. First, in dealing with this problem it is necessary to determine the parameters of the working fluid along the streamlines for multi-stage FP with variable from crown to crown mass flow of the working fluid. The marked change often occurs in the steam turbines FP, where the extraction

of the working fluid is carried out between the stages, for example, for the feed water heating or a heat supply needs.

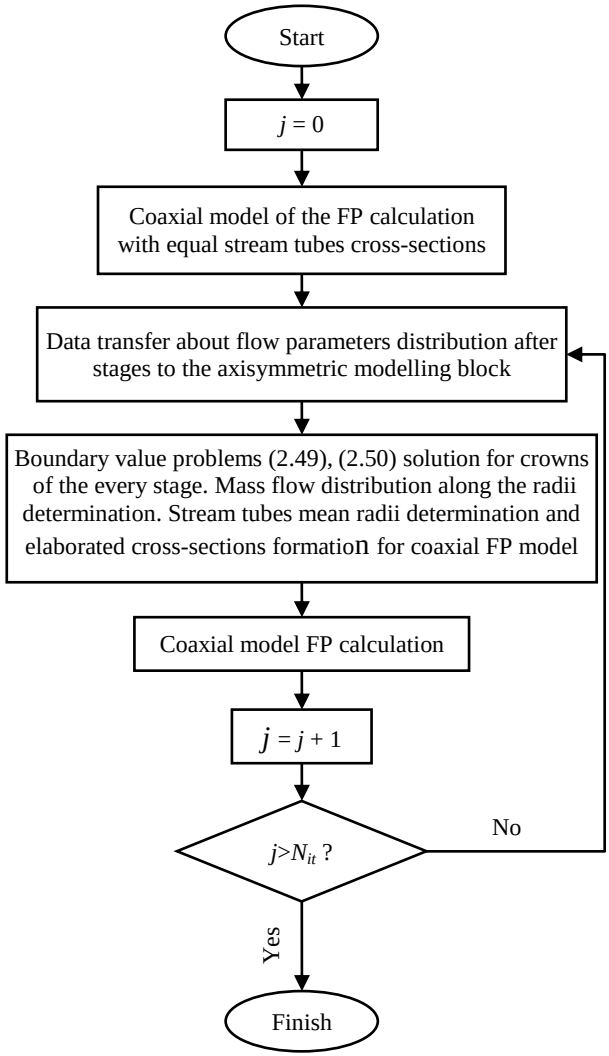

Figure 2.13 *A block diagram of a multistage axial turbine FP axisymmetric problem solving with coaxial models.*

Considering that the equations (2.49) and (2.50), describing axisymmetric flow, valid for one stream line with a constant stream function along it, which value for the single-stage and multi-stage FP without extraction of the working fluid varies from $\Psi = 0$ to $\Psi = G_0 / (2\pi)$, there is a need to adjust the definition of the stream function with the extraction of the working fluid.

In this case, the most appropriate is the idea lies in the fact that the maximum value of the stream function for all crowns drive must be the same. With this in mind, is quite clear the Ψ^* definition

$$\Psi^* = \left(\frac{G_{0(i)}}{2\pi} \right) \Big/ G_{0(i)} = \frac{1}{2\pi}. \tag{2.64}$$

Thus, for the solution of (2.49) and (2.50), the boundary conditions for nozzle and the rotor in this case will be as follows:

$$\begin{cases} r_1(\Psi = 0) = r_{1h}; \quad r_1\left(\Psi = \Psi^* = \dfrac{1}{2\pi}\right) = r_{1t}; \\ r_2(\Psi = 0) = r_{2h}; \quad r_2\left(\Psi = \Psi^* = \dfrac{1}{2\pi}\right) = r_{2t}. \end{cases} \tag{2.65}$$

Numerical integration of the equations (2.49), (2.50) is carried out by the Runge-Kutta third order accuracy method. The algorithm for determining streams tubes mean radii and their cross-sectional areas described below.

Using dependencies $r_1 = r_1(\Psi)$ and $r_2 = r_2(\Psi)$, as result of two-point boundary value problems for nozzle and rotor solutions, define, first of all, the root and tip stream tubes sizes. We assume that the mass flow through the stream tubes will be equal to 1% of the flow through the respective vanes. In this case, the current value of the Ψ function for the mean line of the root stream tube will be equal to

$$\Psi_1 = \Psi^* \cdot 0.005 = \frac{0.005}{2\pi}, \tag{2.66}$$

and for tip stream tube, respectively,

$$\Psi_m = \Psi^* - \Psi_1 = \frac{0.995}{2\pi}. \tag{2.67}$$

Using linear interpolation algorithms on the received values of the stream functions corresponding to the utmost stream tubes mean lines, determine their radii. For other stream tubes the values of the stream functions and the mean line radii will be defined similarly by condition of equal mass flow rates for all stream tubes, which values are determined from the following relationship:

$$g_{(i,\,j)} = 0.98 g_{(i)} (m-2). \tag{2.68}$$

As the result of boundary problems solutions (2.49) and (2.50), the mean radii of stream tubes for all the crowns of multistage FP are transmitted to the coaxial model, where for the new stream tube's cross-sectional areas, angular velocities, and all the geometric characteristics of the nozzle and working blades, the FP calculation is carried out and the new static pressure distribution after working stages crowns is determined.

The FP calculation results using the algorithm corresponding to the coaxial model again transferred to the block of boundary problems solutions (2.49) and (2.50). Described iterative process continues as long as the results of the calculation for both FP calculation algorithms differ less than a prescribed accuracy. Thus, the FP coaxial model and boundary value problems (2.49) and (2.50) complement each other in solving the axisymmetric problem, eliminating the "alignment" on the results of the one-dimensional calculation and more adequately assess the value of disposable heat drop of FP stages.

It should be noted that the numerical implementation of the axisymmetric mathematical model of the working fluid flow in the FP in the form of alternate

use of coaxial mathematical model and boundary problems, can with a high degree of adequacy and accuracy to model the processes in the FP with stages with relatively long blades and having a twisted crowns substantially different from the law $c_u r = \text{const}$. As an example, in Fig. 2.14 are shown the shape of the flow lines resulting from the calculation of LPC FP of powerful steam turbine using the above axisymmetric mathematical model.

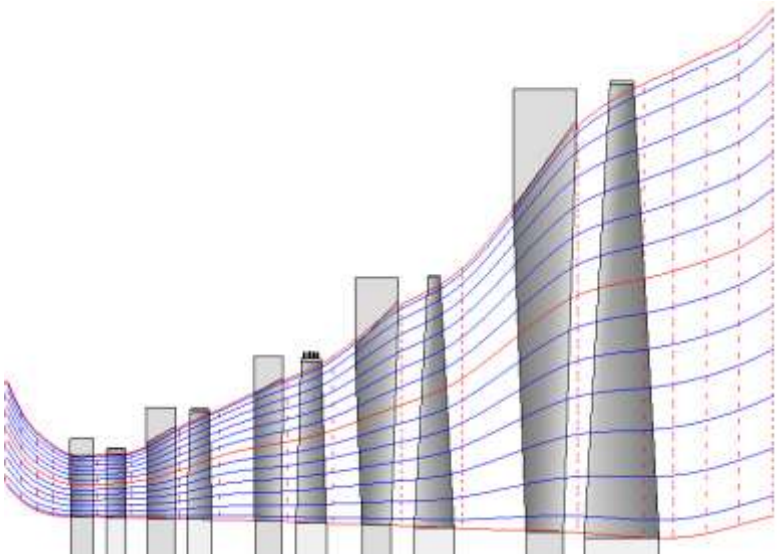

Figure 2.14 *Stream lines of the flow in the powerful steam turbine LPC FP.*

2.2.5 Cascades Flow Calculation

For the design of high efficiency axial flow turbines flow path it is important to have accurate, reliable and fast method for calculation of cascade flow and friction loss on the profile surfaces.

In the calculation of subsonic flows of an ideal liquid in the cascades long used an approach based on the reduction of partial differential equations to Fredholm integral equation of the 1-st or 2-nd kind [8, 22]. Available numerical implementation of solutions to these equations are facing a number of problems

that do not allow a sufficient degree of reliability or accuracy of the calculated arbitrary configuration cascades.

For example, for a long time, we used the method of calculation [22] reduces to the solution of the integral equation of the second kind with respect to the speed potential. It is possible to solve a number of important practical problems of cascade optimization, but had important shortcomings: the complexity of the integral equation kernel normalization, which led to difficulties in calculating thin and strongly curved profiles, as well as the need for numerical differentiation calculated potentials, which brings an additional error in the profile velocity distribution.

Later, we developed a method for cascades potential flow numerical calculating with an approximate view of the ideal gas compressibility based on the solution of the Fredholm equation of the 2-nd kind with respect to speed on the rigid surface, and a program for the PC is designed to work interactively.

Friction loss on the profile is carried out by calculating the compressible laminar, transitional and turbulent boundary layers using one-parameter Loitsiansky method [23]. To improve the accuracy of the results obtained on the basis of the recommendations given in the literature, calculated buckling points and end of the transition from laminar to turbulent boundary layer depending on the pressure gradient, the degree of free-stream turbulence and of profile surface roughness.

The developed algorithms for an ideal fluid flow calculation in the cascade and the boundary layer on the surface of the profile give a good qualitative and quantitative agreement between the calculated and experimental data for different types of cascades at different inlet angles, relative pitch, Mach and Reynolds numbers, characterized by high speed and are therefore suitable for use in problems of optimizing the axial turbomachinery blades shape.

2.2.6 Computational Fluid Dynamics Methods

Aerodynamic optimization of turbine cascades is directed search a large number (hundreds to thousands) variants for their geometry, which increases with the number of variable parameters. The most reliable source of objective data on the flow of gas in a turbine cascade – physical experiment – obviously can not provide a sufficiently deep extreme.

Therefore, currently in the works for aerodynamic optimization it is the most popular approach in which to obtain data on the nature and parameters of the flow of the working fluid in the tested inter-blade channels numerically solve the Navier-Stokes equations, or their modifications [24].

Navier-Stokes equations written in conservative form is as follows:

$$\frac{\partial U}{\partial t}+\frac{\partial F_i}{\partial x_i}+\frac{\partial G_i}{\partial x_i}=B\,, \tag{2.69}$$

where U, F_i, G_i, B – ordered sets of combinations of basic variables

$$U=\begin{bmatrix}\rho\\ \rho V_j\\ \rho E\end{bmatrix};\quad F_i=\begin{bmatrix}\rho v_i\\ \rho v_i v_j+p\delta_{ij}\\ \rho E v_i+p v_i\end{bmatrix};\quad G_i=\begin{bmatrix}0\\ -\tau_{ij}\\ -\tau_{ij}v_j+q_i\end{bmatrix};\quad B=\begin{bmatrix}0\\ \rho F_j\\ \rho F_j v_j\end{bmatrix}.$$

Since the analytical solution of this system of equations associated with insurmountable mathematical difficulties, such a direction as computational fluid dynamics (CFD) arose, which deals with the numerical solution of the Navier-Stokes equations. The numerical solution of the equations of fluid dynamics involves replacing the differential equations of discrete analogs. The main criteria for the quality of the sampling scheme are: stability, convergence, lack of nonphysical oscillations. Computational fluid dynamics is a separate discipline, distinct from theoretical and experimental fluid dynamics and complement them. It has its own methods, its own sphere of applications, and its own difficulties.

Given the speed of modern computers, the most appropriate approach is based on a system of Reynolds-averaged Navier-Stokes (RANS) equations. It involves some additional turbulence modeling using some complimentary to the system (2.69) equations, which are called turbulence model.

The reliability obtained by the CFD results requires a separate analysis. As an example, compare the results of experimental studies of stages with $D/l = 3.6$ (Fig. 2.15–2.17) with the calculations in one-dimensional, axisym-metric (for gaps) and 3*D* CFD statements [19].

Table 2.1 *Main parameters of the test stages.*

Parameter	**Value**	
Stage design	**MI**	**MII**
Inlet pressure, Pa	117000	130000
Inlet temperature, K	373	373
Outlet pressure, Pa	100000	100000
Rotation frequency, 1/s	7311	8212
Nozzle vane mean diameter, m	0.2978	0.2978
Nozzle vane length, m	0.0822	0.0822
Blade mean diameter, m	0.2986	0.2986
Blade length, m	0.0854	0.0854
Nozzle vane outlet gauging angle near hub, deg.	20	17.2
at mean radius, deg.	24	17.5
at peripheral radius, deg.	28	17.8
Blade outlet gauging angle near hub, deg.	32	41
at mean radius, deg.	29.7	26
at peripheral radius, deg.	26	19

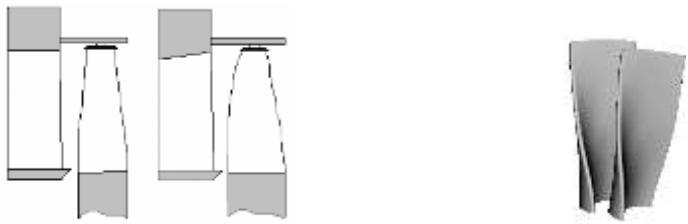

a b

Figure 2.15 *Sketches of MI (left) and MII (right) stage design (a) and stage MI blades (b).*

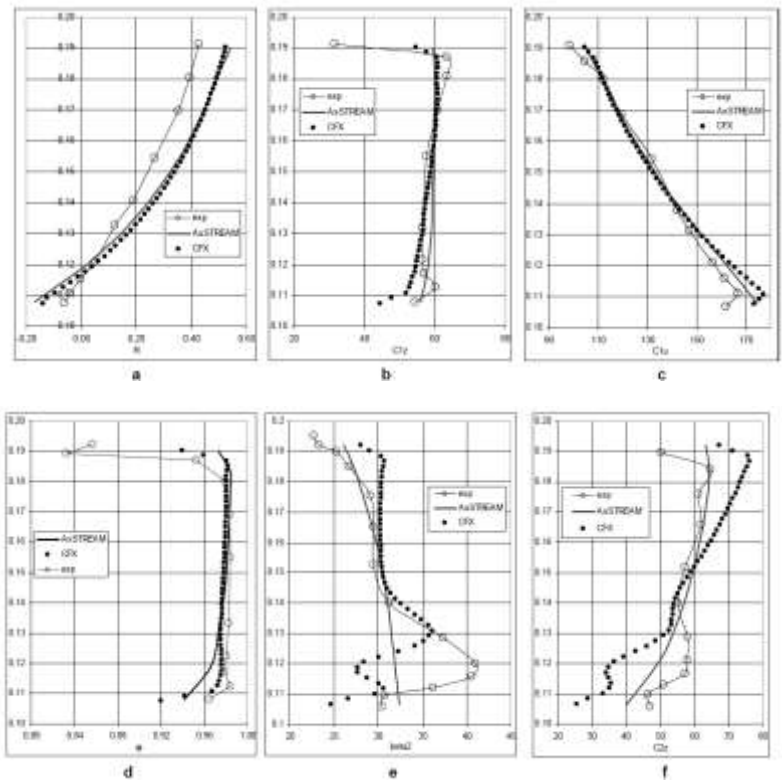

Figure 2.16 *Computation vs experiment (comparison for stage MI).*

Flow parameters distribution along nozzle vane and blade height:

a – reaction; *b* – axial velocity component after nozzle vane;

c – tangential velocity component after nozzle vane; *d* – nozzle vane velocity coefficient; *e* – blade exit flow angle in relative motion; *f* – axial velocity component after blade

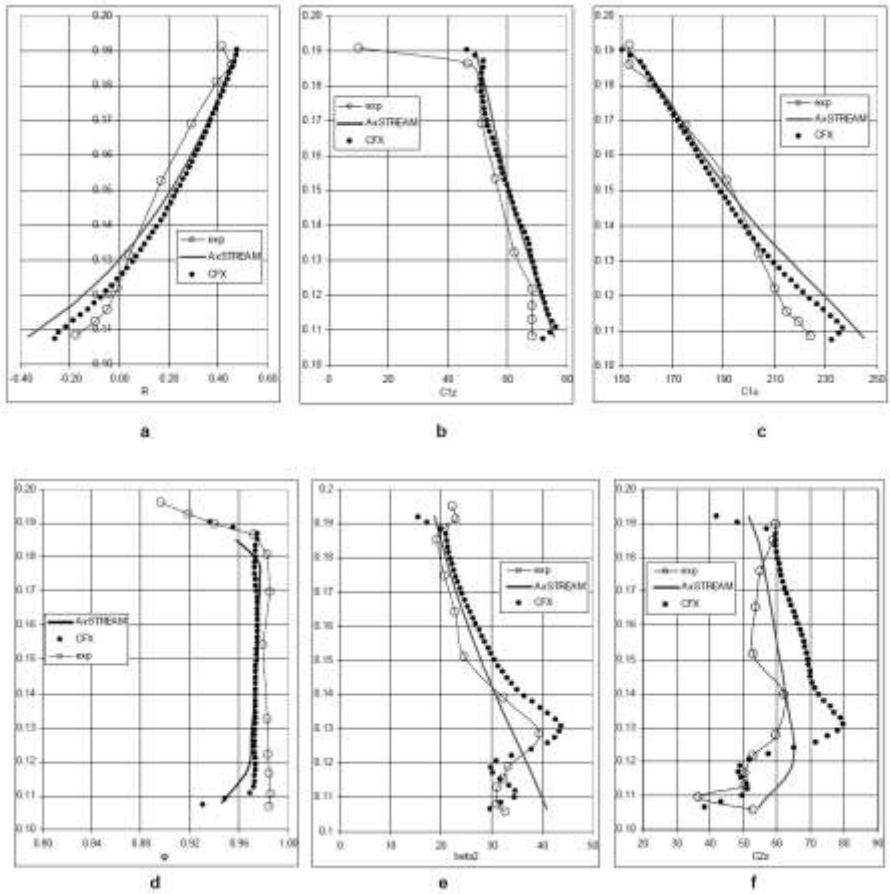

Figure 2.17 *Computation vs experiment (comparison for stage MII).*

Flow parameters distribution along nozzle vane and blade height:

a – reaction; *b* – axial velocity component after nozzle vane;

c – tangential velocity component after nozzle vane; *d* – nozzle vane velocity coefficient; *e* – blade exit flow angle in relative motion;

f – axial velocity component after blade

Table 2.2 *Comparison of stages MI and MII parameters at minimum radial clearance.*

Parameter	Stage MI			Stage MII		
	2*D* AxSTREAM	**3*D* CFX**	**Experiment**	**2*D* AxSTREAM**	**3*D* CFX**	**Experiment**
$(u/C_0)_{opt}$	0.6	0.627	0.62	0.55	0.550	0.55
ξ_s, %	3.5	4.0	2.7	4.9	5.2	3.1
ξ_r, %	2.2	2.1	2.4	2.1	3.0	4.6
ξ_{out}, %	10.8	13.9	11.9	6.8	9.0	7
η_i, %	82.3	80.0	83	84.9	82.8	85.3

It was shown that proper unidimensional and axisymmetric models combined with proven empiric methods of loss calculation provide the accuracy of the turbine flow path computation sufficient for optimization procedures in a bulk of practice valuable cases. Comparative analysis of the experiment and simulation results indicates an untimely nature of the assertion that 3*D* CFD analysis is already capable to substitute physical experiments.

2.3 Geometric and Strength Model

2.3.1 Statistical Evaluation of Geometric Characteristics of the Cascade Profiles

For accurate estimates of the size of the blades, which takes into account not only their aerodynamic properties and conditions of safe operation, it is required to calculate the set of dependent geometric characteristics of the profiles (DGCP) as a function of a number of parameters that determine the shape of the profile. When the shape of the profiles is not yet known, to assess DGCP should use statistical relations. From the literature are known attempts to solve a similar problem [25, 26] on the basis of the regression analysis.

The DGCP include: f – area; I_e and I_n – minimum and maximum moments of inertia; I_u – moment of inertia about an axis passing through the center of gravity of the cross section parallel to the axis of rotation *u*; φ – the angle between the central axis of the minimum moment of inertia and the axis *u*;

X_{gc}, Y_{gc} – the coordinates of the center of gravity; β_i – stagger angle; l_e, l_{ss} – the distance from the outermost points of the edges and suction side to the axis *E*; l_{in}, l_{out} – the distance from the outermost points of the edges to the axis *N*; $W_e, W_{ss}, W_{in}, W_{out}$ – moments of profile resistance.

The listed DGCP values most essentially dependent on the following independent parameters (IGCP) β_{1g} – geometric entry angle; β_{2eff} – effective exit angle; b – chord; t/b – relative pitch; r_1, r_2 – edges radii; ω_1, ω_2 – wedge angles.

Formal macromodelling techniques usage tends to reduce the IGCP number, taking into account only meaningful and independent parameters. In this case, you can exclude from consideration the magnitude of r_1, r_2, ω_2, taking them equal $r_1 = 0.03b$; $r_2 = 0.01b$; $\omega_2 = 0.014K_\omega\omega_1/(0.2+\omega_1)$, $K_\omega = 1...3$, depending on the type of profile [26].

We obtained basic statistical DGCP relationships using profiles class, designed on the basis of geometric quality criteria – a minimum of maximum curvature of high order power polynomials [15] involving the formal macromodelling technique. Approximation relations or formal macromodel (FMM) are obtained in the form of a complete quadratic polynomial of the form (1.2):

$$y(\vec{q}) = A_0 + \sum_{i=1}^{n}(A_i + A_{ii}q_i)q_i + \sum_{i=1}^{n-1}\sum_{j=i+1}^{n} A_{ij}q_iq_j \ .$$

The response function $y(\vec{q})$ values (DGCP) corresponding to the points of a formal macromodelling method, calculated by the mathematical model of cascades profiling using geometric quality criteria.

Analysis of profiles used in turbine building reveals, that two of remaining four IGCP β_{1g} and *t*/*b* highly correlated.

It is advisable to use in place of these factors their counterparts – the flow rotation angle in the cascade θ and the parameter $\Delta t = t/b - T$, where $T = 1.08 - 0.004\theta$ – linear regression equation that specifies the statistical relationship between the relative pitch and angle of rotation of the flow, the resulting data for typical turbine cascade.

Thus, informal macromodelling as IGCP were taken: $\theta, \beta_{2e}, \omega_1, \Delta t$, relatively in ranges 20…120, 10…30, 20…30, –0.2…0.2. In normalized form in the range of –1…1 the factors are calculated as follows:

$$q_1 = \frac{\theta - 70}{50}, \quad q_2 = \frac{\beta_{2e} - 20}{10}, \quad q_3 = \frac{\omega_1 - 25}{5}, \quad q_4 = \frac{\Delta t}{0.2}. \tag{2.70}$$

During macromodelling were designed 25 turbine cascades with $b = 1$ and with IGCP values, corresponding to the points in the of numerical experiment plan, were calculated DGCP values and the dependencies on the form (1.2) built for them. Calculation of flow diagrams and loss factors confirms the high aerodynamic quality of the 25 profile cascades.

In Tables 2.3, 2.4 the FMM coefficients and variance of the cascades DGCP FMM are given. In the tables FMM coefficients increased by 10^4.

Similar relationships were also obtained for a special class of nozzle profiles with an elongated front part [26].

Table 2.3 *DGCP macromodels coefficients.*

A(i, j)	$\ln(F)$	$\ln(I_e)$	$\ln(I_n)$	$\ln(I_u)$	φ	β_i
A(0)	–26530	–87000	–53800	–64034	320	9010
A(1)	4049.2	16769	4241.7	13055	–68.183	–3422.5
A(2)	–45	53.333	37.5	4423.8	–13.683	–1920.8
A(3)	807.5	1200.8	579.17	727.58	–0.5833	–68.333
A(4)	–538.33	–1075	–228.33	–3982.6	83.917	726.67

Table 2.3 *DGCP macromodels coefficients (continuation).*

A(1, 1)	4716.7	6769.2	4024.2	6248.7	–162.02	–1454.6
A(2, 2)	1207.9	2385.4	715.42	1000.2	4.7333	–342.08
A(3, 3)	194.17	711.67	55.418	41.169	–15.867	81.666
A(4, 4)	–204.58	–542.08	–198.33	–1300.1	11.133	186.67
A(1, 2)	562.5	602.5	690	–1472	–120.55	–567.5
A(1, 3)	147.5	–367.5	175	148.5	25.25	–32.5
A(1, 4)	572.5	1412.5	445	1584.8	30.25	–12.5
A(2, 3)	342.5	552.5	180	53	21	–40
A(2, 4)	810	2520	522.5	3917.8	–91.5	–400
A(3, 4)	–7.5	52.5	–2.5	–36.75	–2	12.5

Table 2.4 *DGCP macromodels coefficients (continuation).*

A(i, j)	X_{gc}	Y_{gc}	l_e	I_{ss}	I_{in}	l_{out}
A(0)	2927	5540	1371	882	3726	6090
A(1)	1090.1	–213.75	1093.8	635.14	–63.5	165.75
A(2)	976.42	–657.33	–25.508	–31.008	157.42	–99.667
A(3)	49.417	2.0833	9.2333	47.708	–23.5	26
A(4)	–344.75	237.83	23.558	–32.825	–84.25	61.75
A(1, 1)	433.04	–399.42	324.87	405.3	237.33	–207.75
A(2, 2)	14.292	–135.04	93.692	142.72	–1.2918	–9.8752
A(3, 3)	–30.708	48.583	15.58	19.396	–5.668	9.8748
A(4, 4)	–65.958	34.958	–22.688	–29.929	20.042	18.5
A(1, 2)	–68.75	–500	4.275	51.4	227.5	–241.5
A(1, 3)	19.5	4.75	31.05	29.6	–24.25	19
A(1, 4)	38.5	118	61.825	61.375	–40.25	44.75
A(2, 3)	–5	–10	25.75	22.425	1.5	–3.5
A(2, 4)	192	8.5	79	90.8	35.25	–13.5
A(3, 4)	–6.75	12	5	1.6	5.25	5

2.3.2 Strength Models

On the choice of cascade's optimal gas dynamic parameters significantly affect the strength limitations, which, in turn, is largely dependent on the flow path design.

For example, the calculation of splitted diaphragms strength based on using a simplified scheme, according to which the diaphragm is considered as a semi-circle rod (band with a constant cross-section), loaded with unilateral uniform pressure and supported on the curved outer contour[27]. This approach allows us to evaluate the maximum stress in the diaphragm and is sufficient to assess the strength of the diaphragm at the stage of conceptual and technical design.

Calculation of the blades strength is carried out using the beam theory that restrict computer time to evaluate the tensile and bending stress, for example, using statistical data on profiles, as shown in Section 2.3.1.

To ensure the vibration reliability of blading, rotor blades requires detuning from resonance, i.e., the natural frequencies of the blades should not coincide with the frequency of the disturbing forces that are multiples of the frequency of rotation. The required for detuning dynamic (depending on rotation speed) the first natural frequency of the blade is defined by a simplified formula.

2.4 Flow Path Elements Macromodelling

Macromodels are dependencies of the "black box" type with a reduced number of internal relations. This is most convenient to create such dependence in the form of power polynomials. Obtaining formal macromodels (FMM) as a power polynomial based on the analysis of the results of numerical experiments conducted with the help of the original mathematical models (OMM).

Therefore, the problem of formal macromodelling includes two subtasks:

1. The FMM structure determining.

2. The numerical values of the FMM parameters (polynomial coefficients) finding.

As is known, the accuracy of the polynomial and the region of its adequacy greatly depend on its structure and order. At the same time, obtaining polynomials of high degrees requires analysis of many variants of the investigated flow path elements, which leads to significant computer resources cost and complicates the process of calculating the coefficients of the polynomial.

To create FMM it is advisable to use the mathematical apparatus of the design of experiment theory to significantly reduce the number of computing experiments with OMM, i.e. obtain sufficient information with a minimum dimension of the vector of observations Y'. We use two types of FMM – (1.2) and (1.12). To get them methods of the design of experiment theory applied (three-level Boxing-Benkin plans and saturated Rehtshafner's plans) and cubic spline interpolation.

In a particular implementation of a formal macromodelling methodology need to perform the following steps:

1) the choice of the IMM of the flow path element;

2) the appointment of its performance criteria;

3) choice of OMM parameters, whose influence on performance criteria of the flow path element is necessary to study in detail and the formation on their basis vector of varied parameters $\vec{Q}$;

4) macromodelling area appointment (ranges of components of the vector $\vec{q}$);

5) DOE matrix formation;

6) active numerical experiments conducting and evaluation of the components of observations vector Y' for each criterion;

7) the processing of the experimental results and the determination of the FMM coefficients.

Steps 1–4 are not amenable to formalization and their implementation should take into account the specific features of macromodelling objects and existing experience of designing elements of axial turbines flow path.

2.5 Thermal Cycles Modelling

Imagine the process of analyzing the thermal cycle in the example of gas turbine unit (GTU) (Fig. 2.18) in the following sequence:

- the structure diagram presentation as a set of standard elements and connections between them;
- entering the input data on the elements;
- generation of computer code in the internal programming language based on the chosen problem statement;
- processing;
- post-processing and analysis of results.

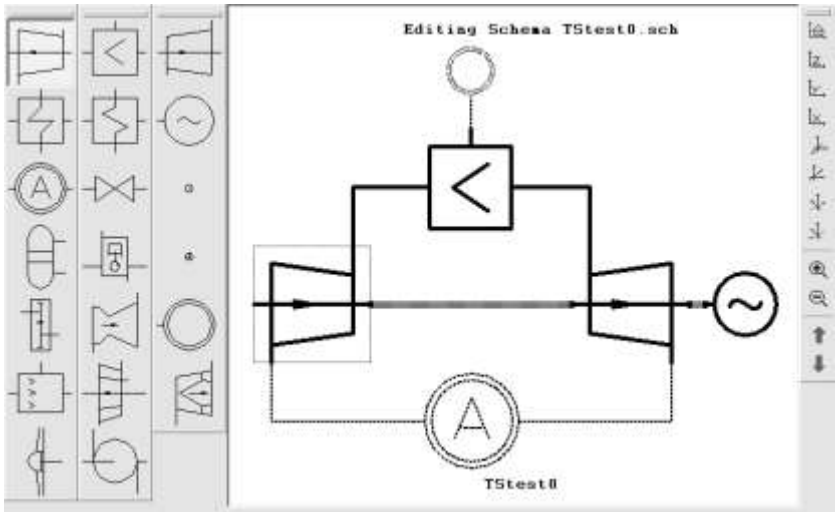

Figure 2.18 *Thermal schemes graphical interactive editor window.*

This sequence of actions combines a high degree of automation of routine operations (input-output and storage of data, programming, presentation of the results of calculations, and so on) with the possibility of human intervention in the process of calculations at any stage (editing of data, changing the program code in the domestic language, writing additional custom code for non-standard calculations performing, etc.).

A key element of the algorithm, allows it to compile a more or less broad class of configurations, is the stage of code generation, based on a graphic description of the scheme (a set of elements and relations between them), i.e., parsing. The problem is that it is pointless to try to solve the problem of the scheme calculation for the arbitrary, sometimes physically implemented schemes. Therefore, the goal of the analyzer is also identification of semantically incorrect scheme descriptions using heuristics embedded in it.

The analyzer's task is to draw up code for solving the system of algebraic equations that describe the problems of cycle analysis in one of the selected language. This system of equations must be linked to energy balances of

different types (for example, flows of working fluids or shafts power) and, therefore, from the graph scheme should provide specific elements chains and use them to make a chain of appropriate formulas. Code generation is based on the information on the scheme chosen by the parser from the internal data structures of elements and connections.

This information includes, in particular, the total number of elements in the cycle, the number of elements of each type, chain elements attached to one shaft, the chain members having regard for air and gas. In addition, there is the total number of connections found and created a list of links with the types and numbers of adjacent elements, as well as the types of energy source. For the efficient operation of the analyzer is required to implement rather complex and flexible dynamic data structure to describe the types and implementation elements, links, as well as types and implementations of data elements and relationships.

Cycle element is an object that is indivisible (in terms of the cycle calculation) for modeling processes of energy conversion and exchange or energy flows. In fact the element is quite complex and multifaceted structure which includes information about the external and the internal representation of its mathematical model, a set of data divided into input and output (and, depending on the type of problem to be solved), a list of associated interface functions etc.

The cycle consists of elements and links between them. Cycle description is stored in a special text file format that contains data by elements, links and service information. Since a sufficiently large number of elements in the scheme, the appointment of links is time-consuming operation, which requires a lot of attention to the formation of the schema file, is desirable to have an interactive graphical schema editor, with which the elements and their relationship just "drawn" on the screen (Fig. 2.18). During the graphical information and elements data input the online preliminary control of the integrity and correctness of the scheme is performed.

Schema data includes collection of data of its elements and links that are relevant to the mathematical modeling of physical processes occurring in the cycle. In connection with this set of data is determined by the requirements of the codes, implementing these models – in our case – a "closed" to the user kernel. External modules available to the user (files of elements and schemes, interpreted code), when changed the set of data of a particular element, should be modified, preferably through means provided by the system or, in extreme cases, manually.

The program of thermal schemes calculation organized in such a way that the graphical user interface and substantive part (solver) would be relatively independent of each other. This makes it possible, on the one hand, to use a solver as a standalone program or as part of other systems, and the other – to connect other solvers to the interface for pre- and post-processing. Therefore solver and interface program have independent data structures.

Solver is a dynamic link library that provides a set of procedures, sufficient for data input and output, as well as organizing the process of setting up and solving the balance equations of thermal cycle. The interpreter has the ability to access these functions, and thus becomes a real calculation procedure described above.

Mathematical modeling of cycles based on predetermined mathematical models of its constituent elements. This approach usually allows to simplify and speed up the calculations. Each of the circuit elements is a more or less complicated object, which can be described with varying degrees of detail.

There are significant differences in the simulation of the elements in the schemes calculation at design and off-design operation modes. In the latter case, the properties of the elements are given as characteristics (maps), i.e. dependency of the output parameters of the regime one. In some cases the characteristics building (especially for the compressors) is a fairly time-consuming task.